

**Ana Filipa Teixeira da Silva**

**Characterization and modulation of survivin in an experimental model of  
pulmonary arterial hypertension**

**Porto, 2013**

**Ana Filipa Teixeira da Silva**

**Master Degree Course in Cardiovascular Pathophysiology**

**Supervisor:** Professor Tiago Henriques Coelho, MD PhD

*To my parents*

*In memory of my godmother*

## ACKNOWLEDGMENTS

The elaboration of this master thesis would not have been possible without those who, with their support, dedication and above all friendship, motivated and helped me overcome the most difficult battles. To all of you I express my sincere gratitude:

To Professor Adelino Leite-Moreira, head of the Department of Physiology and Cardiothoracic Surgery for trusting me and give me the opportunity to grow as student, as scientist and mostly as an individual.

To my supervisor Professor Tiago Henriques Coelho, thank you for all the guidance, scientific experience and support you gave me in all these years. Your enthusiastic spirit and competence were crucial to made me see you as an example to follow. Words are not enough to express how thankful I am.

To my buddy, you have been my coach, my scientific “big brother” and my example during this journey. Thank you for all the help, support and courage you gave me. Thank you for all the laughs we shared but also for all the “I told you so...” that I needed to hear. Hope our friendship remains for the upcoming years even knowing that I am your “qualified slave”. Everybody should know a person like you.

To my friend Nádia Gonçalves, I know you don't like acknowledgements but I am so thankful for all the friendship you provided me in such short period of time. Thank you for all advises and encouragement words you gave me, they were crucial for me to grow. Also thank you for all the excessive hours of work we had together, they were full of amazing treasures that I will never forget.

To Manuel Pinto, for all the hours of work and dedication to this project we had together. It has been an amazing journey with you. Even when we don't agree we make the best team.

To Joana Justino, Paulo Silva and Sara Pinto you make the lab a special place to be. Thank for all the hours of fun and work we have spent together.

To Rita Ferreira and Ana Padrão for all the amazing work we have developed.

To all the staff in the Physiology department with special thanks to Marta Oliveira, Mizé Mendes, Miss Rosinha, Miss Francelina and Miss Margarida.

And lastly...

À minha família, em especial aos meus pais por todo o apoio, carinho e motivação que me deram durante mais esta etapa. Obrigado por caminharem ao meu lado e acreditarem nos meus sonhos mesmo com todas as dificuldades que a vida nos coloca. Tenho os melhores pais do mundo!

Thank you...

## RESUMO

Na última década, estudos sobre a fisiopatologia da Hipertensão Arterial Pulmonar (HAP) demonstraram o papel crucial da remodelagem vascular, observando-se uma mudança do interesse da comunidade científica para a pesquisa de terapias anti-remodelagem. A remodelagem vascular pulmonar pode refletir um desequilíbrio entre mitógenos e inibidores de crescimento, com consequente desregulação da apoptose e proliferação celular. A fase inicial da HAP é geralmente caracterizada por apoptose a nível endotelial enquanto que a fase tardia é caracterizada por resistência à apoptose a nível da íntima e da média. Deste modo, os doentes com HAP em fases precoces beneficiariam de terapias anti-apoptóticas, enquanto que doentes em estadios avançados beneficiariam de estratégias pró-apoptóticas. Neste sentido, avaliar o estado apoptótico de doentes com HAP ajudaria a individualizar terapias. Desta forma, a presente dissertação teve como objetivo caracterizar a expressão das proteínas da via intrínseca da apoptose, survivina e Smac/DIABLO, durante as fases precoce e tardia da HAP induzida pela monocrotalina (MCT). Avaliamos também *in vivo* os efeitos de uma estratégia pró-apoptótica usando terameprocol (TMP), um antagonista da survivina, num modelo experimental de HAP induzido por MCT. Os resultados obtidos demonstram que o aumento da expressão de survivina e a diminuição de Smac/DIABLO, tanto a nível cardíaco como pulmonar, precedem as manifestações hemodinâmicas da HAP, sugerindo fortemente uma causa neurohumoral ao invés de uma dependente da carga. Verificamos ainda que o tratamento com TMP resultou na reversão dos parâmetros hemodinâmicos e histológicos nos animais com hipertensão pulmonar. Concluindo, os dados deste estudo sugerem que a modulação da apoptose pela via da survivina poderá ter um duplo efeito benéfico através da reversão da remodelagem vascular pulmonar e da hipertrofia cardíaca.

**Palavras-chave:** Hipertensão Arterial Pulmonar; apoptose; survivina; Smac/DIABLO; terameprocol.

## ABSTRACT

Over the last decade, research on the pathophysiology of Pulmonary Arterial Hypertension (PAH) highlighted the crucial role of vascular remodeling in its pathophysiology, with a shift in the interest of scientific community to seek anti-remodeling therapies rather than new vasodilators. According to this recent paradigm, pulmonary vascular remodeling might reflect an imbalance between mitogens and growth inhibitors with a deregulation on apoptosis and cell proliferation. Early-stages of PAH are characterized by endothelial apoptosis and late-stages of PAH by apoptosis resistance in both intimal and medial layers. Therefore, patients in early-stages of PAH would benefit from anti-apoptotic therapies whereas patients in advanced stages might benefit from pro-apoptotic strategies. In this context, assessing the apoptosis status would help on individualizing therapies for PAH patients. The present work aimed to characterize the expression of intrinsic apoptotic pathway proteins survivin and Smac/DIABLO during early and late stages of monocrotaline (MCT)-induced PAH. We also evaluated the *in vivo* effect of a pro-apoptotic strategy using terameprocol (TMP), a survivin antagonist, in a MCT-induced model of PAH. Results demonstrate that survivin upregulation and Smac/DIABLO downregulation at cardiac and pulmonary levels preceded hemodynamic manifestations of PAH, strongly suggesting a neurohumoral cause rather than a load-dependent one. We also verified that TMP treatment resulted in reversion of hemodynamic and histological parameters in pulmonary hypertensive rats. In conclusion, our data suggest that targeting survivin in PAH could have dual beneficial effects, by reversing pulmonary vascular remodeling as well as cardiac hypertrophy.

**Keywords:** Pulmonary Arterial Hypertension; apoptosis; survivin; Smac/DIABLO; terameprocol.

# LIST OF CONTENTS

ACKNOWLEDGMENTS .....	V
RESUMO .....	VI
ABSTRACT .....	VII
FIGURE INDEX .....	X
TABLE INDEX.....	XII
LIST OF ABBREVIATIONS .....	XIII
Part I – Introduction .....	15
1. Pulmonary arterial hypertension .....	16
1.1. Definition .....	16
1.2. Classification .....	16
1.3. Epidemiology.....	18
1.4. Pathophysiology.....	18
1.4.1. Genetics .....	19
1.4.2. PAH as panvasculopathy .....	19
1.4.3. Inflammation .....	21
1.4.4. Right ventricular hypertrophy.....	21
1.5. Experimental models.....	22
1.5.1. Monocrotaline model.....	22
2. Apoptosis in PAH.....	23
2.1. The role of apoptosis in pulmonary vascular remodeling.....	25
2.2. Apoptosis as therapeutic target for PAH.....	25
2.2.1. Survivin.....	26
2.2.1.1. <i>Terameprocol</i> .....	28
Part II – Aims.....	29
Part III – Material and Methods .....	45
3. Experimental Design .....	33
3.1. Survivin expression in the progression of MCT-induced PAH.....	33
3.2. Terameprocol in vivo study .....	33
4. Hemodynamic analysis.....	33
5. Tissue Preparation .....	34
6. Morphometric analysis .....	34
7. Immunohistochemistry .....	35
8. Western Blotting .....	35



9. Statistical Analysis.....	36
Part IV – Results.....	37
10. Progression of MCT-induced pulmonary arterial hypertension .....	38
10.1. Right ventricle hemodynamic evaluation .....	38
10.2. Morphometric analysis .....	38
10.3. Survivin and Smac/DIABLO expression .....	42
11. Terameprocol <i>in vivo</i> study .....	45
11.1. Regression of RV dysfunction in MCT animals treated with TMP .....	45
11.2. Terameprocol reverts pulmonary and cardiovascular remodelling .....	46
Part V – Discussion.....	49
Part VI – Conclusions .....	52
Part VII – References.....	54

## FIGURE INDEX

**Figure 1. PAH as panvasculopathy.** In PAH several alterations occur in the 3 layers (adventitia, media and intima) of pulmonary arteries. PAH: Pulmonary Arterial Hypertension; SMC: Smooth muscle cell; EC: Endothelial cell; TGF: Transforming Growth Factor; PDGF: Platelet-derived Growth Factor. .... 20

**Figure 2. Apoptosis pathways.** Two major pathways are present during apoptosis: the extrinsic (or death receptor pathway) and the intrinsic (or mitochondrial pathway). In the extrinsic pathway the activation of death receptors leads to the formation of death inducing signalling complex (DISC) and activation of procaspase-8, initiating the caspase cascade. In the intrinsic pathway, the death stimuli leads to opening of the mitochondrial permeability transition pore (MPT) and thus to the release of cytochrome c and Smac/DIABLO. Cytochrome c will, together with Apaf-1 and procaspase-9, form the apoptosome and activate caspase cascade while Smac/DIABLO will suppress inhibitor of apoptosis proteins (IAPs) thus contributing to caspase activation and apoptosis. Finally the balance between pro and anti-apoptotic Bcl proteins will determine the mitochondrial response to death stimuli. FADD: Fas-associated death domain protein; TRADD: Tumor necrosis factor receptor type 1-associated death domain protein. .... 23

**Figure 3. Roles of survivin.** Survivin is the only inhibitor of apoptosis protein (IAP) known for its double function in inhibiting apoptosis and regulating cell division. Survivin is capable of inhibiting caspases either directly or indirectly (in association with XIAP). Also Smac/DIABLO release suppresses survivin activity. In respect to cell cycle, survivin can be located in the mitotic spindle and the centromeres where in association with proteins Aurora B, Borealin and INCENP regulate chromosome segregation. .... 27

**Figure 4. Experimental design.** Progression of MCT-induced PAH and Terameprocol "in vivo" studies. MCT: Monocrotaline; PAH: Pulmonary arterial hypertension; sc: subcutaneous; DMSO: Dimethyl sulphoxide hybri-max; TMP: Terameprocol; ip: intraperitoneal. .... 32

**Figure 5. Pulmonary arterial hypertrophy.** A) Histological appearance of small pulmonary arteries stained with hematoxylin and eosin; B) Percentage of arterial medial layer hypertrophy. Sham: Sham group; MCT: monocrotaline group. Data are mean±SEM; \*p < 0.05 vs. Sham of the same day, <sup>b</sup>p < 0.05 vs. D7 of the same treatment group, <sup>c</sup>p < 0.05 vs. D3 of the same treatment group, <sup>d</sup>p < 0.05 vs. D1 of the same treatment group. .... 41

**Figure 6. Pulmonary survivin and Smac/DIABLO expression** (A and B, respectively) evaluated by western blot. Sham: sham group, MCT: monocrotaline group. Data are mean±SEM. \*p < 0.05 vs. Sham of the same day, <sup>b</sup>p < 0.05 vs. D7 of the same treatment group. .... 42

**Figure 7. Survivin expression in the right ventricle** evaluated by immunohistochemistry (A and B) and by western blot (C) during the progression of pulmonary arterial hypertension. Sham: Sham group, MCT:

monocrotaline group. Data are mean±SEM. \*p < 0.05 vs. Sham of the same day, <sup>b</sup>p < 0.05 vs. D7 of the same treatment group, <sup>d</sup>p < 0.05 vs. D1 of the same treatment group..... 43

**Figure 8. Smac/DIABLO expression in the right ventricle** evaluated by immunohistochemistry (A and B) and by western blot (C) during the progression of pulmonary arterial hypertension. Sham: Sham group, MCT: monocrotaline group. Data are mean±SEM. \*p < 0.05 vs. Sham of the same day, <sup>d</sup>p < 0.05 vs. D1 of the same treatment group..... 44

**Figure 9. Terameprocol effects on RV maximal pressure and cardiac output** (A and B, respectively). Sham: Sham group, MCT: monocrotaline group, TMP: Terameprocol, CO: cardiac output, P<sub>max</sub>: maximum pressure. Data are mean±SEM. <sup>a</sup>p < 0.05 vs. Sham+V, <sup>β</sup>p < 0.05 vs. Sham+TMP and <sup>γ</sup>p < 0.05 vs. MCT+V. .... 45

**Figure 10. Terameprocol effects on the right ventricle structure** demonstrated by right ventricle/body weight ratio (RV/BW) and cardiomyocyte cross sectional area (CSA) (A and B respectively). Sham: Sham group, MCT: monocrotaline group, TMP: Terameprocol. Data are mean±SEM. <sup>a</sup>p < 0.05 vs. Sham+V, <sup>β</sup>p < 0.05 vs. Sham+TMP and <sup>γ</sup>p < 0.05 vs. MCT+V..... 47

**Figure 11. Pulmonary response to Terameprocol** evaluated by lung weight/body weight ratio (L/BW) and by the percentage of medial hypertrophy of pulmonary arteries (B, A and C respectively). Sham: Sham group, MCT: monocrotaline group, TMP: Terameprocol. Data are mean±SEM. <sup>a</sup>p < 0.05 vs. Sham+V, <sup>β</sup>p < 0.05 vs. Sham+TMP and <sup>γ</sup>p < 0.05 vs. MCT+V..... 48

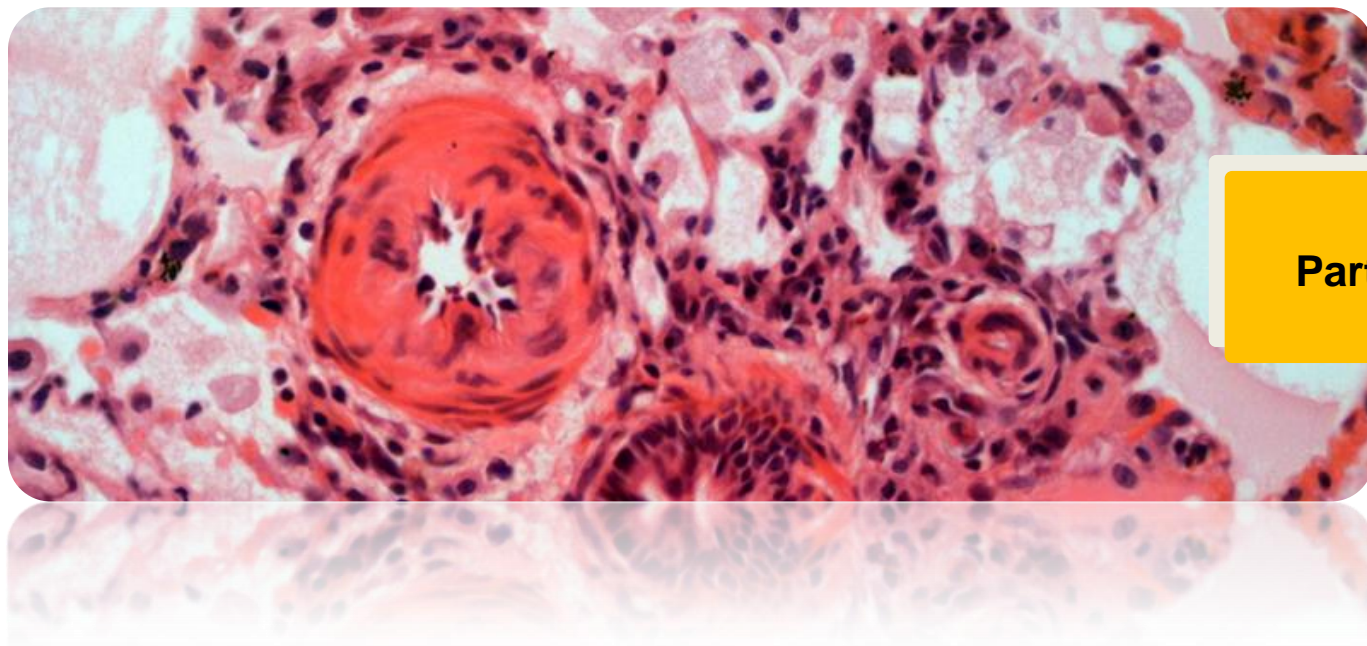
## TABLE INDEX

<b>Table 1.</b> WHO classification of pulmonary hypertension, Dana Point, 2008 .....	17
<b>Table 2.</b> Functional classification of pulmonary arterial hypertension (adapted <sup>7</sup> ).....	18
<b>Table 3.</b> Right ventricle hemodynamic evaluation parameters.....	39
<b>Table 4.</b> Morphometric progression of MCT-induced PAH.....	40
<b>Table 5.</b> Terameprocol effects on cardiac hemodynamics .....	46
<b>Table 6.</b> Effects of Terameprocol in morphometric characteristics.....	47

## LIST OF ABBREVIATIONS

<b>AT</b>	- Angiotensin
<b>AVD</b>	- Apoptotic volume decrease
<b>BIR</b>	- Baculovirus IAP repeat
<b>BMP</b>	- Bone morphogenetic protein
<b>CTEPH</b>	- Chronic thromboembolic pulmonar hypertension
<b>DCA</b>	- Dichloroacetate
<b>DISC</b>	- Death-inducing signalling complex
<b>DMSO</b>	- Dimethyl sulphoxide hybri-max
<b>ECG</b>	- Electrocardiogram
<b>EC</b>	- Endothelial cell
<b>ET-1</b>	- Endothelin-1
<b>EPR-1</b>	- Effector cell proteasereceptor-1
<b>GLUT4</b>	- Glucose transporter protein 4
<b>HAP</b>	- Hipertensão Arterial Pulmonar
<b>HF</b>	- Heart failure
<b>HIF-1<math>\alpha</math></b>	- Hypoxia inducible factor 1- $\alpha$
<b>IAP</b>	- Inhibitor of apoptosis
<b>Ip</b>	- Intraperitoneal
<b>IPAH</b>	- Idiopathic pulmonary arterial hypertension
<b>Kv1.5</b>	- O <sub>2</sub> -sensitive K <sup>+</sup> channel
<b>LV</b>	- Left ventricle
<b>MCT</b>	- Monocrotaline
<b>MH</b>	- Medial Hypertrophy
<b>MPT</b>	- Mitochondrial permeability pore
<b>NDGA</b>	- Nordihydroguaiaretic acid
<b>NFAT</b>	- Nuclear factor of activated T cells
<b>NO</b>	- Nitric oxide
<b>PA</b>	- Pulmonary artery
<b>PAEC</b>	- Pulmonary artery endothelial cell
<b>PAH</b>	- Pulmonary arterial hypertension
<b>PAP</b>	- Pulmonary arterial pressure
<b>PASMC</b>	- Pulmonary artery smooth muscle cell
<b>PCH</b>	- Pulmonary capillary hemangiomatosis
<b>PDE5</b>	- Phosphodiesterase 5
<b>PDGF</b>	- Platelet growth factor

<b>PDH</b>	- Pyruvate dehydrogenase
<b>PDK</b>	- Pyruvate dehydrogenase kinase
<b>PH</b>	- Pulmonary hypertension
<b>PPH</b>	- Primary pulmonary hypertension
<b>PVOD</b>	- Pulmonary veno-occlusive disease
<b>PVR</b>	- Pulmonary vascular resistance
<b>ROS</b>	- Reactive oxygen species
<b>RV</b>	- Right ventricle
<b>RVH</b>	- Right ventricle hypertrophy
<b>Sc</b>	- Subcutaneous
<b>SNP</b>	- Single nucleotide polymorphisms
<b>SSc</b>	- Schistosomiasis
<b>TGF</b>	- Transforming growth factor
<b>TMP</b>	- Tetra-O-methyl nordihydroguaiaretic acid (terameprocol)
<b>VSMC</b>	- Vascular smooth muscle cell
<b>WHO</b>	- World health organization



## Part I – Introduction

## **1. Pulmonary arterial hypertension**

### **1.1. Definition**

Pulmonary arterial hypertension (PAH) is clinically defined as mean pulmonary arterial pressure (PAP) elevation above 25 mmHg at rest or above 30 mmHg with exercise with a mean pulmonary capillary wedge pressure of less than 15 mmHg<sup>1</sup>. PAH is also characterized by vascular growth and proliferation, leading to increased vascular resistance and right heart failure<sup>2</sup>.

### **1.2. Classification**

In 1981 German physician and pathologist Ernest Van Romberg described a case of right heart failure (HF) without a reason for pulmonary arteriosclerosis<sup>1</sup> but it was only in 1951 that Dresdale and colleagues<sup>3</sup> first used the term primary pulmonary hypertension (PPH). An epidemic increase of pulmonary arterial hypertension (PAH), attributed to the excessive use of appetite suppressing drug aminorex fumarate, led to the first World Health Organization (WHO) symposium in 1973 in Geneva<sup>4</sup>, where PH was divided in two categories: PPH, a rare disease with unknown cause and secondary PH, when a disorder is due to known underlying cause and risk factors<sup>5</sup>. Since then, several conferences on PH have been held. The “Evian classification” (2<sup>nd</sup> WHO symposium, Evian, France) in 1998 attempted to classify PH according to its pathological, clinical and therapeutic features. Later in 2003, the 3<sup>rd</sup> WHO symposium was held in Venice, Italy, where the most notable difference was the replacement of PPH in favour of idiopathic pulmonary arterial hypertension (IPAH), familial PAH (when exists a family history of PAH) or associated PAH (when another cause is present such presence of human immunodeficiency virus)<sup>6</sup>. The most recent classification was achieved in 2008 at the 4<sup>th</sup> WHO symposium (Dana Point, California) where familial PAH was replaced by heritable PAH and left heart disease was subdivided in systolic and diastolic dysfunction as well as valvular disease. More recently, in March 2013 the 5<sup>th</sup> WHO Symposium was realized in Nice (France) however the new guidelines have not been published yet.

Currently, PH is clinically classified in: i) PAH; ii) pulmonary veno-occlusive disease (PVOD) and/or pulmonary capillary hemangiomatosis (PCH); iii) PH owing to left heart disease; iv) PH owing to lung diseases and/or hypoxia; v) chronic thromboembolic PH (CTEPH); vi) PH with unclear multifactorial mechanisms (Table 1).



**Table 1. WHO classification of pulmonary hypertension, Dana Point, 2008**

<b>Group I. Pulmonary arterial hypertension (PAH)</b>
1.1. Idiopathic PAH
1.2. Heritable
1.2.1. BMPR2
1.2.2. ALK1, endoglin (with or without hereditary hemorrhagic telangiectasia)
1.2.3. Unknown
1.3. Drug- and toxin-induced
1.4. Associated with:
1.4.1. Connective tissue diseases
1.4.2. HIV infection
1.4.3. Portal hypertension
1.4.4. Congenital heart diseases
1.4.5. Schistosomiasis
1.4.6. Chronic haemolytic anemia
1.5. Persistent pulmonary hypertension of the newborn
<b>Group I'. Pulmonary veno-occlusive disease (PVOD) and/or pulmonary capillary haemangiomatosis (PCH)</b>
<b>Group II. Pulmonary hypertension owing to left heart disease</b>
2.1. Systolic dysfunction
2.2. Diastolic dysfunction
2.3. Valvular disease
<b>Group III. Pulmonary hypertension owing to lung diseases and/or hypoxia</b>
3.1. Chronic obstructive pulmonary disease
3.2. Interstitial lung disease
3.3. Other pulmonary diseases with mixed restrictive and obstructive pattern
3.4. Sleep-disorder breathing
3.5. Alveolar hypoventilation disorders
3.6. Chronic exposure to high altitude
3.7. Developmental abnormalities
<b>Group IV. Chronic thromboembolic pulmonary hypertension (CTEPH)</b>
<b>Group V. Pulmonary hypertension with unclear multifactorial mechanisms</b>
5.1. Hematologic disorders (myeloproliferative disorders, splenectomy)
5.2. Systemic disorders (sarcoidosis, pulmonary Langerhans cell histiocytosis)
5.3. Metabolic disorders (glycogen storage disease, Gaucher disease, thyroid disorders)
5.4. Others (tumoral obstruction, fibrosing mediastinitis, chronic renal failure on dialysis)
BMPR2 – bone morphogenetic protein receptor-II; ALK1 – activin receptor-like kinase 1; HIV – human immunodeficiency virus

Besides the clinical classification, PH patients can also be classified according to their functional performance (Table 2.). This classification has been adopted from the New York Heart Association (NYHA) for left heart disease and together with clinical classification can be useful for diagnosis, prognosis and therapy of PH.

**Table 2. Functional classification of pulmonary arterial hypertension (adapted<sup>7</sup>)**

<b><u>Class I</u></b>	Patients with pulmonary hypertension without resulting in limitation of physical activity. Normal physical activity does not cause undue dyspnoea or fatigue, chest pain or near syncope.
<b><u>Class II</u></b>	Patients with pulmonary hypertension resulting in slight limitation of physical activity. Patients comfortable at rest, but normal physical activity causes undue dyspnoea or fatigue, chest pain or near syncope.
<b><u>Class III</u></b>	Patients with pulmonary hypertension resulting in marked limitation of physical activity. Patients comfortable at rest, but less than normal physical activity causes undue dyspnoea or fatigue, chest pain or near syncope.
<b><u>Class IV</u></b>	Patients with pulmonary hypertension with inability to carry out any physical activity without symptoms. These patient manifest signs of right heart failure. Dyspnoea and/or fatigue may even be present at rest. Discomfort is increased by any physical activity.

### 1.3. Epidemiology

The incidence and prevalence of PAH, respectively, are estimated at 2.4-7.6 cases per million per year and 15-26 cases per million in large population studies<sup>8,9</sup>. Young adults are the most affected being more than two thirds women<sup>10</sup>. This female predominance might be explained by the low survival rate of male fetuses with PPH<sup>11</sup>. However, it is hard to appraise the global prevalence because it depends on the method of diagnosis and the specific groups of population studied. The worldwide prevalence of PAH is likely greater than is recognized given the newer associations with dialysis<sup>12</sup> and metabolic syndrome<sup>13</sup> as well as with the developing world diseases that are risk factors for PAH such as HIV, schistosomiosis and sickle cell disease<sup>14</sup>. However, non-PAH are increasingly far more common.

### 1.4. Pathophysiology

The normal pulmonary circulation is a low-pressure, low-resistance and high-capacitance system (pulmonary vascular resistance being less than one-tenth of systemic vascular resistance) where arteries are compliant structures with few muscle fibers. PAH is characterized by excessive pulmonary vasoconstriction and vascular remodeling that commonly affects all vessel layers (intima, media and adventitia) rising pulmonary vascular resistance (PVR) and PAP ultimately increasing right ventricular afterload. The histological findings in PAH include intimal thickening, medial hypertrophy (MH), adventitial proliferation/fibrosis, arterial occlusion, thrombosis *in situ* and infiltration of inflammatory/progenitor cells<sup>15, 16</sup>. In the later stage of the disease, the formation of a vessel “neointima” is characterized by augmented deposition of extracellular matrix and myofibroblasts. Moreover, located downstream from occluded arteries, plexiform lesions can predominate and express growth factors typically observed in

angiogenesis<sup>17</sup>. It is still unknown the exact processes that initiate the pathological changes observed in PAH however the interaction of predisposing conditions and exogenous stimuli may represent the causes.

#### 1.4.1. Genetics

The study of genetic predisposition of PAH is of utmost importance for the understanding pathogenesis of this disease. Mutations in bone morphogenetic protein (BMP) receptor-2 (BMPR2) are present in more than 70% of familial PAH and 10%-40% of IPAH leading to loss of Smad signalling and therefore to increased proliferation and decreased differentiation of pulmonary artery smooth muscle cells (PASMCs)<sup>18-20</sup>. In spite of the autosomal dominant inheritance of BMPR2 gene mutations, this disease has a low penetrance since only approximately 20% of individuals carrying the mutation will develop PAH<sup>20</sup>.

More research is currently being performed to find possible epigenetic mechanisms that enhanced PAH susceptibility, namely single nucleotide polymorphisms (SNP). SNP variants, including K<sub>v</sub>1.5<sup>21</sup>, transient receptor potential (Trp) channels<sup>22</sup> and serotonin (5-HT) transporters<sup>23</sup>, may predispose to PAH.

#### 1.4.2. PAH as panvasculopathy

Accompanied by the histological features previously described, PAH is currently viewed as a panvasculopathy (Figure 1). In PAH the vasodilator/vasoconstrictor ratio is decreased in the endothelium<sup>24-26</sup> whereas prothrombotic factors, such as tissue factor<sup>27</sup>, are increased. Apoptosis in early stages of PAH may generate apoptosis-resistant endothelial cells (ECs) that cross-talk with PASMCs through growth factors (e.g. transforming growth factor- $\beta$ , TGF- $\beta$ ) leading to EC and fibroblast transdifferentiation and PASMCs proliferation<sup>28</sup>, eventually forming plexiform lesions<sup>29</sup>. Besides growth factors, several other phenomena drive PASMCs into excessive proliferation including: mitochondrial abnormalities<sup>29</sup>, increased expression/activity of platelet-derived growth factor (PDGF) receptor<sup>30</sup> and serotonin receptor (SERT)<sup>31, 32</sup>, tyrosine kinase activation<sup>33</sup> and decreased expression of voltage-gated O<sub>2</sub>-sensitive potassium channel, K<sub>v</sub>1.5<sup>34</sup>. Moreover, metalloproteinase activation causes disruption of the adventitia which allows cell migration and generates mitogenic peptides<sup>35</sup>. Furthermore, adventitial fibroblasts show a hyperproliferative phenotype in PAH, displaying increased sensitivity to 5-HT<sup>36</sup>.

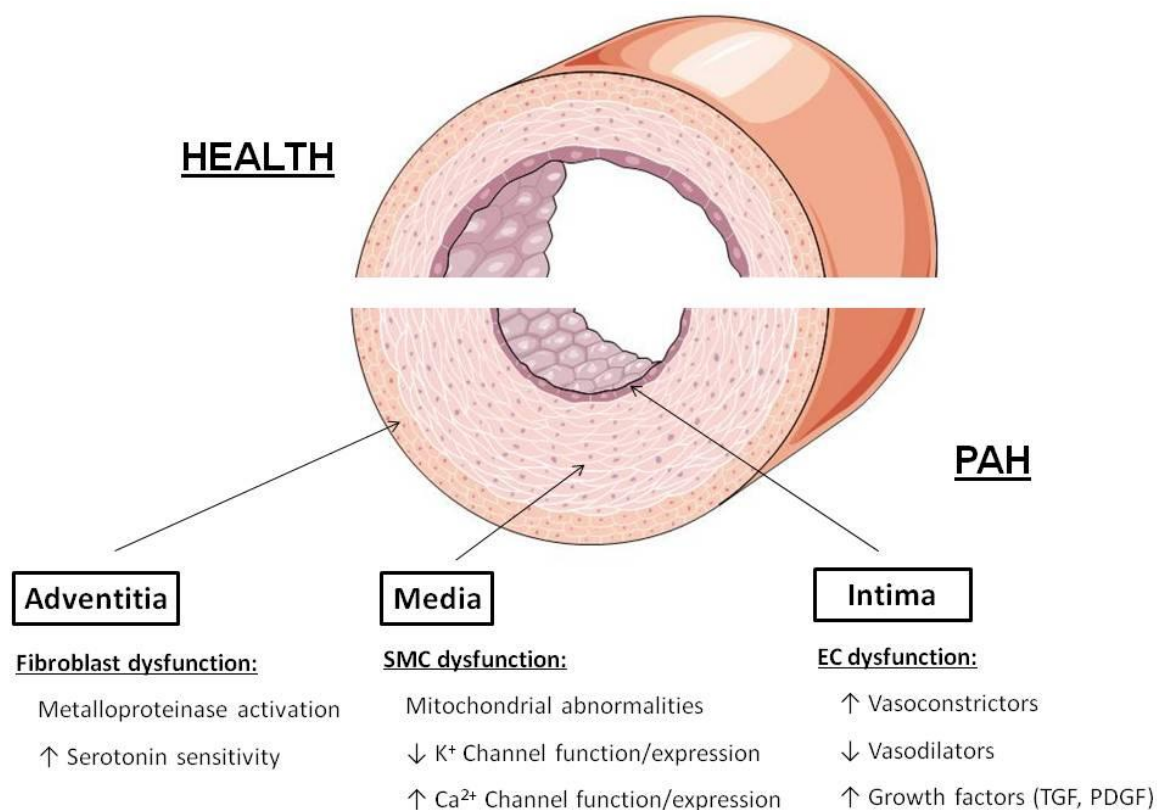


**Figure 1.** PAH as panvasculopathy. In PAH several alterations occur in the 3 layers (adventitia, media and intima) of pulmonary arteries. PAH: Pulmonary Arterial Hypertension; SMC: Smooth muscle cell; EC: Endothelial cell; TGF: Transforming Growth Factor; PDGF: Platelet-derived Growth Factor.

Several observations indicate that PAH shares a mitochondrial-metabolic abnormality with cancer, the “Warburg phenotype”, a shift in glucose metabolism from oxidative phosphorylation to glycolysis (despite adequate oxygen supply) that enhances proliferation and prevents apoptosis<sup>37</sup>. The downstream consequences of this mitochondrial-metabolic abnormality include mitochondrial hyperpolarization, reduced production of reactive oxygen species (ROS), normoxic-activation of hypoxia inducible factor-1 $\alpha$  (HIF-1 $\alpha$ ), overexpression of pyruvate dehydrogenase kinase (PDK) and decreased expression K<sub>v</sub>1.5 channels<sup>37</sup>. Other groups demonstrated that these mitochondrial abnormalities can be partially reverted by Dichloroacetate (DCA), a PDK inhibitor and K<sub>v</sub>1.5 channel opener. Indeed, DCA activates pyruvate dehydrogenase (PDH), increasing glucose oxidation, restoring mitochondrial membrane potential and reversing normoxic HIF-1 $\alpha$  activation<sup>37</sup>.

### 1.4.3. Inflammation

Increasing attention is being focused on several inflammatory mechanisms that play a key role in experimental models of PAH and in human PAH. These include the presence of T and B cells monocytes, macrophages and dendritic cells in plexiform lesions<sup>38, 39</sup>, the detection of autoantibodies on ECs and fibroblasts<sup>40</sup>, raised cytokine and chemokine levels<sup>41</sup> and the association of PAH with certain infections such as human herpes virus 8 (HHV-8)<sup>42</sup> and HIV<sup>43</sup>. The nuclear factor of activated T cells (NFAT) is known for increasing the transcription of multiple inflammatory mediators such as interleukins (IL) and tumour necrosis factor- $\alpha$  (TNF- $\alpha$ )<sup>44</sup>. Activation of NFAT in PAH causes the downregulation of K<sub>v</sub>1.5<sup>45</sup> and regulates the transcription of several genes that control mitochondrial function<sup>46</sup>. Moreover, NFAT was also found to be activated in PASMCs isolated from patients with PAH and that inhibition of its predominant isoform, NFATc2, would contribute to attenuate monocrotaline(MCT)-induced PAH<sup>47</sup>.

Finally, PAH is associated with latent viral infections (such as HIV and HHV-8) and schistosomiasis (SSc). Nonhuman primates infected with chimeric simian HIV-nef virus demonstrated lung vascular remodeling characteristic of PAH<sup>48</sup>. Moreover, the HIV-nef gene was also implicated in plexiform lesions in pulmonary arteries of HIV-infected patients with PAH<sup>49</sup>. SSc, a parasitic infection that causes inflammation and pulmonary vascular disease, has also been implicated in PAH. Infiltration of T and B cells together with increased levels of IL-6, CX3CL1 and RANTES have been reported in the pulmonary vascular lesions of PAH patients with SSc<sup>6</sup>. Additionally mice chronically infected with SSc presented extensive pulmonary vascular remodeling in the absence of PH and correlated with cytokine IL-13 levels<sup>50</sup>.

### 1.4.4. Right ventricular hypertrophy

One of the consequences of PVR increasing is right ventricular overload leading to right ventricular hypertrophy (RVH) and failure. According to the Laplace relationship an elevated intraluminal pressure leads to an increase in wall stress, unless the chamber wall thickness is increased or the internal radius of the chamber is reduced. To compensate the high pressure registered in PAH, the right ventricle (RV) adapts by increasing wall thickness and assuming a more rounded shape<sup>51</sup>. The increase in ventricular mass is due to myocyte hypertrophy, sarcolemmal and contractile protein synthesis, altered calcium homeostasis, a shift in gene expression and extracellular matrix remodelling<sup>52</sup>. Although is known that the best approach to reduce RVH is to treat the underlying pulmonary arterial alterations, recent data suggests that RV can be an independent target in experimental PAH<sup>53</sup>. For exemple, inhibition of phosphodiesterase 5 (PDE5) (e.g. sildenafil) improved RV contractility<sup>53</sup>, without altering left ventricle (LV) function.

In normal conditions the RV is capable of adjusting its substrate utilization from fatty acids to glucose. In RVH the myocardium is reliant on anaerobic glucose metabolism due to PDK activation and it has hibernating properties, demonstrating augmented glucose oxidation and contractility in response to DCA<sup>54</sup>.

Studies in MCT-induced PAH have demonstrated an upregulation of glucose transporter protein 4 (GLUT4)<sup>55</sup>.

Moreover alterations in neurohumoral signalling, formation of ROS as well as nitrogen species and exaggerated inflammatory responses can also lead to right heart failure<sup>51</sup>. Still, more research is needed on therapy agents with effects on both RV and pulmonary vasculature.

## 1.5. Experimental models

Even though animal models do not mimic all the characteristics of human pathology, they have allowed the study on several diseases and its therapeutics<sup>56</sup>. Until now, no animal model has been able to mimic all the biochemical and histopathological features of PAH<sup>57</sup>. MCT and hypoxia are the most frequently used animal models in the study of this disease<sup>56</sup>. Although MCT model has been used for over than 50 years, the molecular mechanisms underlying MCT-induced PAH have yet to be better clarified<sup>58</sup>.

### 1.5.1. Monocrotaline model

Derived from the seeds of *Crotalaria spectabilis*, monocrotaline (MCT) is a toxic pyrrolizidine alkaloid that can be administrated by intraperitoneal (60 mg/Kg), subcutaneous (60 mg/Kg), or intravenous injection (1-5 mg/Kg) inducing vascular injury after hepatic generation of its pyrrolic derivative by cytochrome P450 3A<sup>59</sup>. With a single injection of MCT rats develop PAH after approximately 3 weeks and die within 6-8 weeks<sup>60</sup>, making this a very simple and thus technically appealing animal model available to a wide spectrum of investigators. Unfortunately, MCT represents a significant limitation for long-term survival studies because it can injury other organs like the liver<sup>61</sup> and the kidney<sup>62</sup>. Another limitation is the different sensitivity that rat strains present to MCT<sup>63</sup> which may be related to the pharmacokinetics of this molecule<sup>59</sup>. MCT primarily affects the pulmonary arterial bed because lungs are the first major vascular bed after the liver<sup>64</sup>. In fact, at the pulmonary level, the ECs are the first site of damage. After only 4h of MCT administration rats develop platelet thrombi in small arteries<sup>65</sup> and within 4 days EC toxicity by increasing the number of swollen mitochondria and decreasing the proportion of microfilaments<sup>66, 67</sup>. Approximately 7 days after MCT injection there is a peripheral extension of SMCs into small nonmuscularized PAs<sup>66</sup> and an increase in oxygen consumption and cardiac index<sup>68</sup>. The medial hypertrophy of small PAs is described 12 days post MCT injection accompanied by an increase in PAP. RVH is only present later in the disease<sup>68</sup> (~21 days after injection) together with increased RV systolic and diastolic pressures and ultimately RV failure<sup>69-71</sup>.

## 2. Apoptosis in PAH

The pathogenesis of PAH is a complicated, multifactorial process. The current vasodilator therapies are limited and research is now pursuing strategies that could reverse structural remodeling in the pulmonary arterial bed, thus providing a more significant decrease in PVR. Even though growth is the classical mechanism associated with vascular remodeling, it has increasingly been acceptable that apoptosis may influence the extent of alterations that occurs<sup>72</sup>. Indeed, a reduction in apoptosis has been implicated in severe PAH while induction of this mechanism seems to promote the regression of pulmonary vascular remodeling.

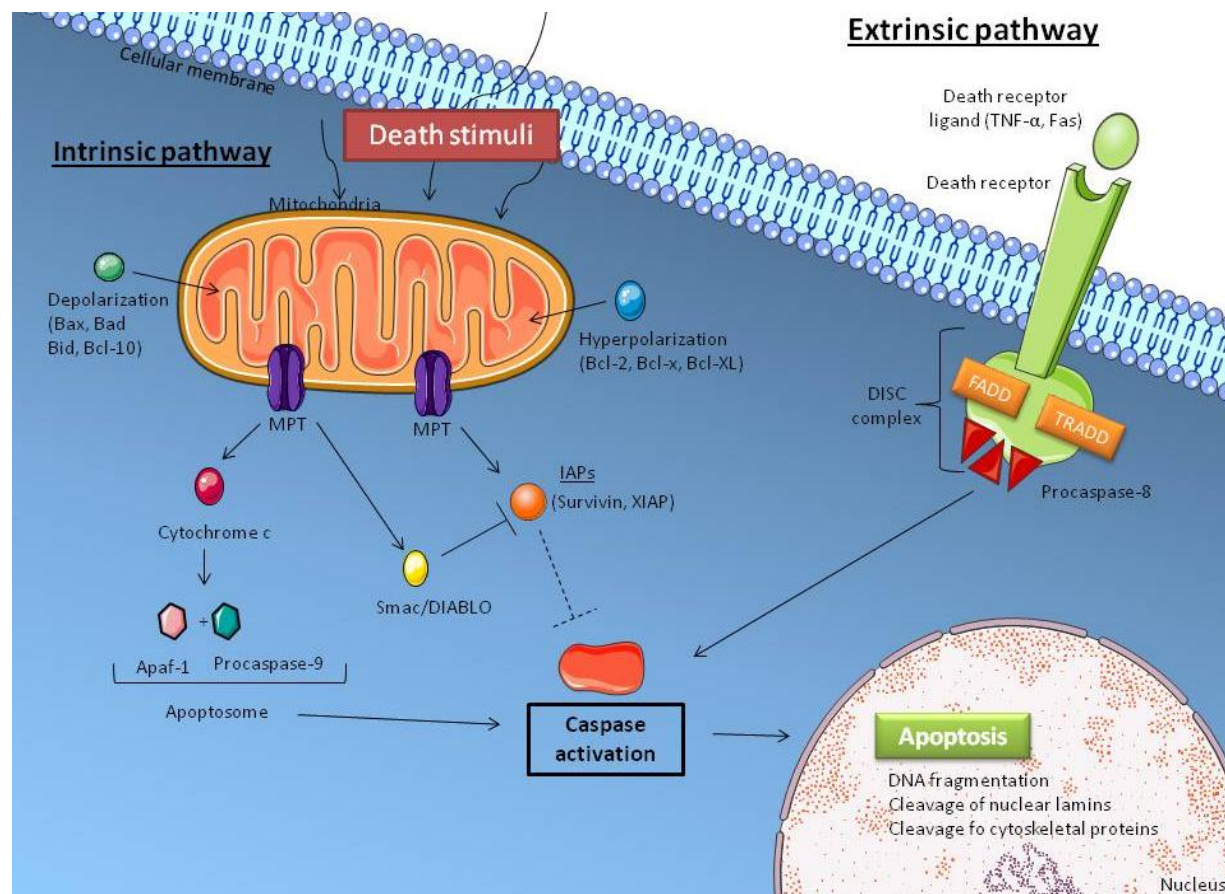


**Figure 2. Apoptosis pathways.** Two major pathways are present during apoptosis: the extrinsic (or death receptor pathway) and the intrinsic (or mitochondrial pathway). In the extrinsic pathway the activation of death receptors leads to the formation of death inducing signalling complex (DISC) and activation of procaspase-8, initiating the caspase cascade. In the intrinsic pathway, the death stimuli leads to opening of the mitochondrial permeability transition pore (MPT) and thus to the release of cytochrome c and Smac/DIABLO. Cytochrome c will, together with Apaf-1 and procaspase-9, form the apoptosome and activate caspase cascade while Smac/DIABLO will suppress inhibitor of apoptosis proteins (IAPs) thus contributing to caspase activation and apoptosis. Finally the balance between pro and anti-apoptotic Bcl proteins will determine the mitochondrial response to death stimuli. FADD: Fas-associated death domain protein; TRADD: Tumor necrosis factor receptor type 1-associated death domain protein.

Apoptosis, or programmed cell death, is an important biological process of normal tissue development and function that involves the genetically determined elimination of cells. It is characterized by a distinct series of morphological and biochemical alterations such as cell shrinkage, chromatin condensation, DNA fragmentation, caspase activation, formation of apoptotic bodies and membrane blebbing<sup>73-75</sup>. The apoptotic events are initiated when the cells loss their volume upon the receiver of apoptotic signals (Figure 2). Then mitochondrial membrane potential is depolarized, cytochrome c (cyt c) is released and caspases are activated. Finally, the last phase is when the DNA degradation occurs, apoptotic bodies are formed, the nuclear lamina and cytoskeleton are degraded and the internal phosphatidyl serine is exposed to the external environment.

Until now, two major apoptotic pathways are known: the intrinsic or mitochondrial pathway and the extrinsic or death receptor pathway. Both pathways converge on the same execution phase that involves the activation of specific cysteiny aspartic acid-proteases (caspase-3, caspase-6 and caspase-7). These activate cytoplasmic endonucleases and proteases that degrade nuclear and cytoskeletal material<sup>76</sup>. The extrinsic pathway initiates apoptosis through transmembrane receptor-mediated interactions involving death receptors and ligands that are members of the TNF receptor gene superfamily<sup>77</sup> like FasR/FasL, TNFR1/TNF- $\alpha$ /, DR3/Apo3L/, DR4/Apo2L and DR5/Apo2L<sup>78-82</sup>. Upon ligand binding cytoplasmic adapter proteins, such as FADD and TRADD, are recruited and associated with procaspase-8 via dimerization of the death effector domain. This leads to the formation of a death-inducing signalling complex (DISC) that activates procaspase-8<sup>83</sup>. After that, the execution phase begins with the activation of caspase-8. The intrinsic pathway can be initiated through either negative signalling (absence of factors that suppress death programs such as growth factors, hormones and cytokines) or positive signalling (radiation, toxins hypoxia, hyperthermia, viral infections and free radicals). Both signals lead to loss of the mitochondrial transmembrane potential, formation of the mitochondrial permeability transition pore (MPT) and release of pro-apoptotic proteins such as cytochrome c and Smac/DIABLO from the intermembrane space to the cytosol<sup>84</sup>. Once released into cytosol, cytochrome c binds and activates Apaf-1 and procaspase-9 to form the “apoptosome”<sup>85, 86</sup> which then activates caspase-9 and lead to chromatin degradation and apoptosis. Although the exact mechanisms are yet to be discovered, thoughts are that Bcl-2 family of proteins is the responsible for the regulation of apoptotic mitochondrial events<sup>87</sup>. This family of proteins is constituted by either pro-apoptotic proteins (Bcl-10, Bax, Bak, Bid, Bad, Dim, Bik and Blk), that upon mitochondrial transmembrane potential depolarization regulate cytochrome c release<sup>88</sup>, and anti-apoptotic proteins (Bcl-2, Bcl-x, Bcl-XL, Bcl-XS, Bcl-w and BAG) that can promote mitochondrial hyperpolarization and prevent both the opening of MPT and release of cytochrome c<sup>89</sup>.

In addition, ion channels are known to perform an essential role in apoptosis. High concentration of intracellular K<sup>+</sup> ([K<sup>+</sup>]<sub>i</sub>) is needed to maintain a normal cell volume. Opening of plasma membrane voltage-gated K<sup>+</sup> channels increases the loss of cytoplasmic K<sup>+</sup> inducing apoptotic volume decrease (AVD). On the other hand, closure or downregulation of K<sup>+</sup> channels contributes to the maintenance of [K<sup>+</sup>]<sub>i</sub> attenuating



apoptosis<sup>90, 91</sup>. Moreover  $[K^+]_i$  is also required for the suppression of caspases and nucleases in the final apoptotic stage<sup>91</sup>.

Finally, the last component of apoptosis is the phagocytic uptake of apoptotic bodies where the externalization of phosphatidylserine onto the outer leaflet facilitates noninflammatory phagocytic recognition leading to an early uptake and disposal<sup>92</sup>.

## 2.1. The role of apoptosis in pulmonary vascular remodeling

Recent research demonstrated that apoptosis has an important pathophysiological role in PAH by eliminating unwanted cells such as cells migrated into the vascular lumen and hypertrophied cells accumulated in the pulmonary vasculature<sup>93</sup>.

Apoptotic modulators in the vasculature are diverse and include ROS<sup>94</sup>, NO<sup>95</sup>, angiotensin type 2 (AT2) receptors<sup>96</sup> and the endothelin system<sup>97</sup>. For example, ROS are involved in PAH and more specifically in H<sub>2</sub>O<sub>2</sub> induced-apoptosis of vascular cells by PKC dependent mechanism<sup>98</sup>.

Animal studies demonstrated that inducing apoptosis of hypertrophied PASMC in intact pulmonary vasculature can prevent the progression of the medial hypertrophy<sup>93, 99, 100</sup>.

Moreover, apoptosis of hypertrophied PASMCs has been related to a regression in medial hypertrophy while inhibition of apoptosis is related to progression of pulmonary vascular medial thickening<sup>100-102</sup>. This assumption is based on the theory for a spatio-temporal diversity within the vascular wall as PAH progresses. In this theory, an inherited or acquired alteration in BMP axis promotes the apoptosis of pulmonary artery endothelial cells (PAECs) and consequently loss of small capillaries (constituted essentially by PAECs tubes) leading to the increase of the flow and shear stress in the remaining vessels. Intima cell proliferation and plexiform lesions are formed with the emergence of apoptosis-resistant PAECs expressing survivin<sup>29</sup>. Simultaneously, the loss of PAECs expose PASMCs to circulating growth factors such PDGF that has been shown to induce the expression of survivin<sup>103</sup> and thus a resistance to apoptosis. Although all of this knowledge, the role of apoptosis in the pulmonary vascular remodeling needs further research. Studies on the mechanisms and biochemical markers of apoptosis will help in the understanding the role of apoptosis has a treatment for PAH.

## 2.2. Apoptosis as therapeutic target for PAH

Discover that normal vascular smooth muscle cells (VSMCs) possess the machinery to undergo apoptosis allowed the assumption that this phenomenon may be the one responsible for regulating cell number in the vessel wall.<sup>104</sup> While early PAH is characterized by increased apoptosis in the endothelial layer, late disease is characterized by suppressed apoptosis and increased proliferation both in intima and media. Therefore an anti-remodeling treatment may be a potential therapeutic option against various types of PAH.

Patients in early stages of PAH may benefit from an antiapoptotic strategy, whereas the ones in late forms of PAH may receive a pro-apoptotic approach.

### 2.2.1. *Survivin*

Inhibitors of apoptosis (IAPs) are a family of proteins related with apoptosis. Several mammalian IAP family members have been identified including, NIAP<sup>105</sup>, c-IAP1 and 2, X-IAP<sup>106</sup>, apollon, TX-XIAP, livin, survivin and bruice.<sup>107-109</sup>

Survivin is a IAP known for its double function as inhibitor of apoptosis and regulator of cell division<sup>110</sup> (Figure 3.). This protein was first discovered in 1997 by Ambrosini and colleagues while hybridization screening of a human genomic library with cDNA of the effector cell protease receptor-1 (EPR-1)<sup>111</sup>. Survivin presents a high homology to EPR-1 and has been mapped to chromosome 17 at band 25 encoding a protein of 142 amino acids, with a molecular weight of approximately 16.3 kDa<sup>111</sup>. The initial studies revealed a strong survivin expression in fetal tissues whereas little or no survivin was detected in normal adult tissues<sup>110, 112-115</sup>. Interestingly, this protein is known to be expressed in most cancers and it is described as the fourth most significant transcriptome expressed in human tumors<sup>116</sup>. The feature that defines apoptosis in the IAP protein family members is the presence of baculovirus IAP repeat (BIR) in at least one copy. Inhibition of proteolytic maturation and enzyme activity of caspases by IAPs may be due to a physical association with initiator and effector caspases<sup>114, 117</sup>. In fact, several IAPs BIRs act as caspases-interacting regions. The dual function that separates survivin from the other IAP family members is ensured by its unique structure. Since this protein presents only one copy of a modified BIR domain similar to the three-dimensional structure BIR3 domain of XIAP. Survivin is thought to be able to interact with XIAP, protecting it from ubiquitination and increasing its stability leading to caspase-9 inhibition<sup>118, 119</sup>. This interaction was also studied through HeLa cells in which loss of phosphorylation of threonine 34 by p34<sup>cdc2</sup>-cyclin B1 leads to dissociation of an immunoprecipitable survivin-caspase-9 complex on the mitotic apparatus and thus caspase-9-dependent apoptosis<sup>119</sup>. Moreover, expression of the T34A dominant-negative mutant has shown a depletion of procaspase-9 in culture tumor cell lines<sup>120</sup>.

Despite direct binding between survivin and the caspases has not been confirmed, survivin may also inhibit caspase activity indirectly through the mitochondrial pathway of apoptosis.

Mitochondrial pro-apoptotic dimeric protein Smac/DIABLO is known for increasing Apo-2L/TRAIL-induced caspase-3 activity and thus suppress the activity of survivin and other IAPs such XIAP and cIAP1<sup>121</sup>. During mitochondrial apoptosis pathway Smac/DIABLO along with cytochrome c are released from mitochondria into the cytosol promoting apoptosis. This is due to the suppression of inhibitor effects of the IAP proteins<sup>122</sup>. Concluding, the binding of Smac/DIABLO to survivin leads to its delayed release in the cytosol, which in turn results in prolonged cell survival<sup>123</sup>.

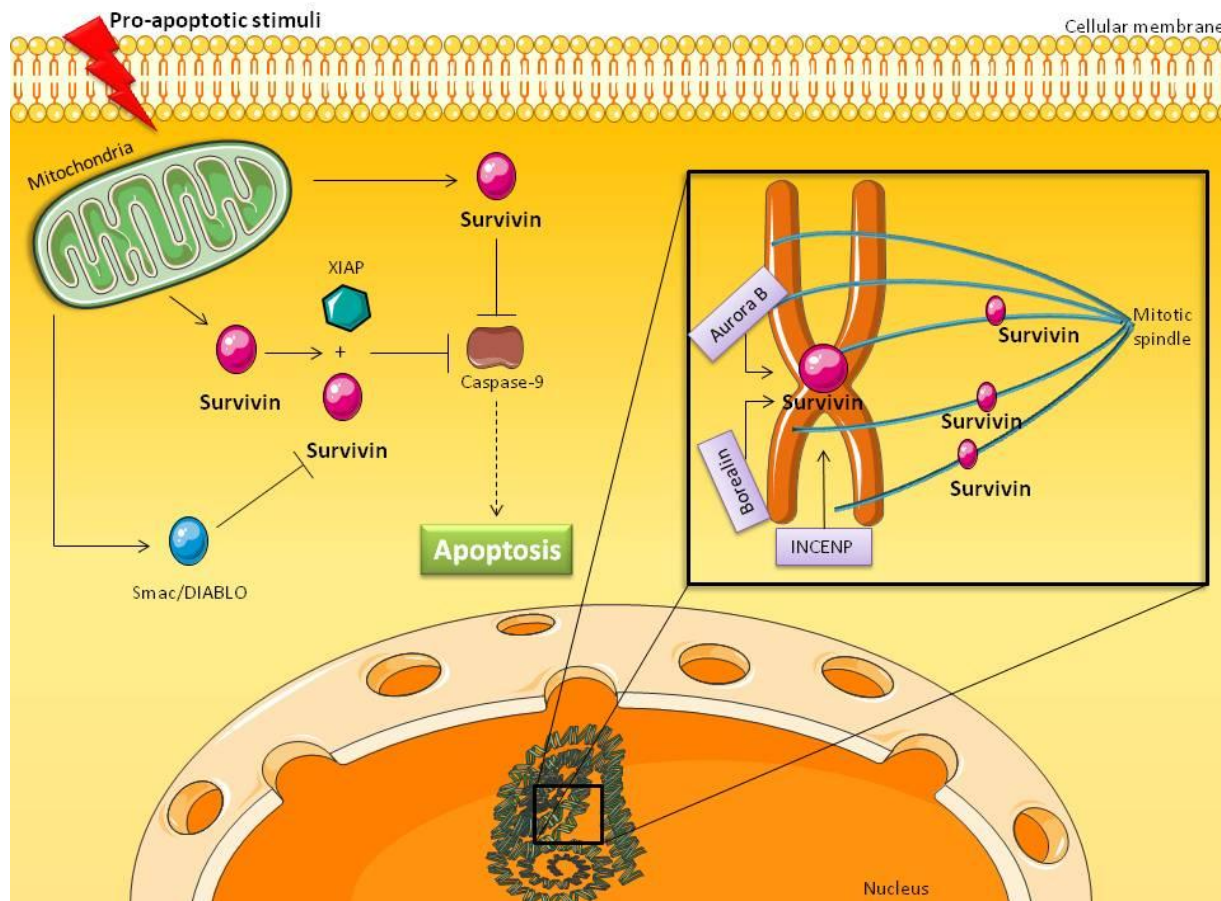


**Figure 3. Roles of survivin.** Survivin is the only inhibitor of apoptosis protein (IAP) known for its double function in inhibiting apoptosis and regulating cell division. Survivin is capable of inhibiting caspases either directly or indirectly (in association with XIAP). Also Smac/DIABLO release suppresses survivin activity. In respect to cell cycle, survivin can be located in the mitotic spindle and the centromeres where in association with proteins Aurora B, Borealin and INCENP regulate chromosome segregation.

Most IAP family members are considered anti-apoptotic proteins, however the gene that encodes survivin (BIRC5) generates five major isoforms of the transcript by alternative splicing: survivin-2 $\alpha$  and survivin-2B that favour induction of apoptosis as well as survivin- $\Delta$ Ex3, survivin-3B and wild type (WT)-survivin that appear to be cytoprotective<sup>124-126</sup>. Survivin is the only IAP protein capable of regulating cell division by interacting with the mitotic apparatus by binding to microtubules through its C-terminal domain<sup>127</sup>. In fact its expression is present on centromeres at prophase/metaphase and in the spindle midzone during anaphase/telophase<sup>128, 129</sup>. Survivin recognizes phosphorylated histone H3 associating with the chromosome passenger proteins Aurora B, INCENP and the neoformed complex is recruited to the centromeres to ensure a proper chromosomal segregation<sup>130</sup>. Moreover, survivin is present in centrosomes of dividing cells where it binds to Cdk1 which after activation allows cells to enter mitosis<sup>119</sup>. It has been proposed that survivin has multiple compartmentalizations in the cells that include the nucleus, the cytoplasm and the mitochondria<sup>118, 131, 132</sup>. Nuclear localization seems to be connected to the ability of survivin to regulate cell cycle by facilitating progression and inducing exit of the cells from G1 checkpoint

arrest and subsequent entry into S phase<sup>133-135</sup>. The greatest stability of survivin happens in the mitochondria where it is associated with oncogenic transformation, possibly increasing protection from apoptosis in cancer cells. This survivin confers resistance to apoptosis by inhibiting activation of effector caspases<sup>118, 132</sup>. Once apoptosis is initiated survivin exit the mitochondria and remains in cytoplasm where it loses its cytoprotective ability, probably because posttranslational modifications occur<sup>136</sup>. Finally, it was recently described that stress stimuli leads to a release of survivin to the cytosol, retaining both anti-apoptotic and proliferative actions<sup>137-139</sup>. It is believe that the increased release of mitochondrial survivin to cytoplasm and sequestering of Smac/DIABLO are of the utmost importance for the apoptosis resistant phenotype of neoplastic cells. This findings lead to the thought that use of molecular antagonists of survivin to increase cell death and prevent pathological resistance to apoptosis might hold therapeutic potential.

#### 2.2.1.1. Terameprocol

Terameprocol (tetra-O-methyl nordihydroguaiaretic acid, M4N, EM1421, TMP) is a hydrophobic molecule derivated of the nordihydroguaiaretic acid (NDGA) isolated from the plant *Larrea tridentata*<sup>140, 141</sup>, known for obliterating survivin gene expression<sup>142, 143</sup> by binding to the transcription factor Sp1. *In vitro* studies demonstrate that terameprocol induced apoptosis and growth arrest of various human cancer cell lines<sup>142-148</sup>. *In vivo* experiments with murine models of human xenograft solid tumors demonstrated the anti-tumoral action of this compound with no relevant systemic toxicity<sup>143-147</sup>. Moreover, clinical trials are already initiated to evaluate the potential of TMP in diverse types of neoplasias and also in the prevention of sexually transmitted viruses.

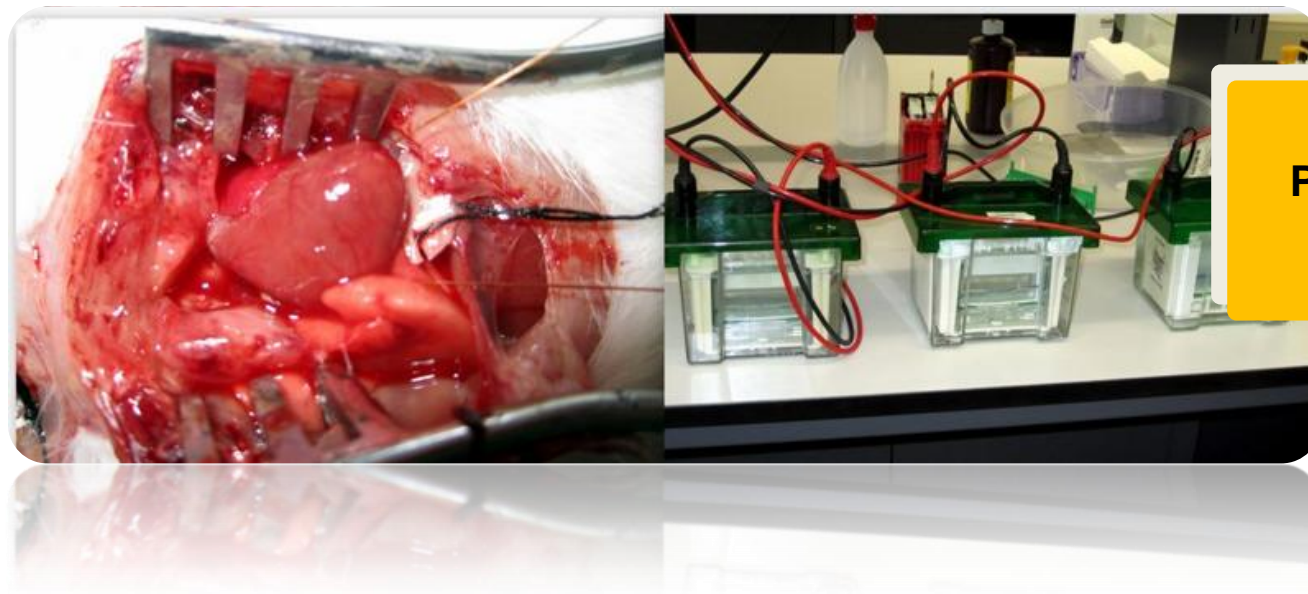


**Part II – Aims**

Considering the concepts reviewed before, the aim of the present study was to investigate the contribution of apoptosis to the pathogenesis of PAH through the analysis and modulation of the anti-apoptotic protein survivin in an animal model of MCT induced-PAH.

In order to achieve the objective the work was divided in two parts, namely:

- a) Survivin expression in the progression of MCT-induced PAH
  - Pulmonary and cardiac patterns of controls and animals with MCT-induced PAH were related with expression of survivin and Smac/DIABLO proteins throughout the hemodynamic and morphometric progression of disease;
- b) Terameprocol *in vivo* study
  - The effects of terameprocol *in vivo* administration were characterized through morphometric and hemodynamic evaluation of sham and pulmonary hypertensive rats.



### **Part III – Material and Methods**

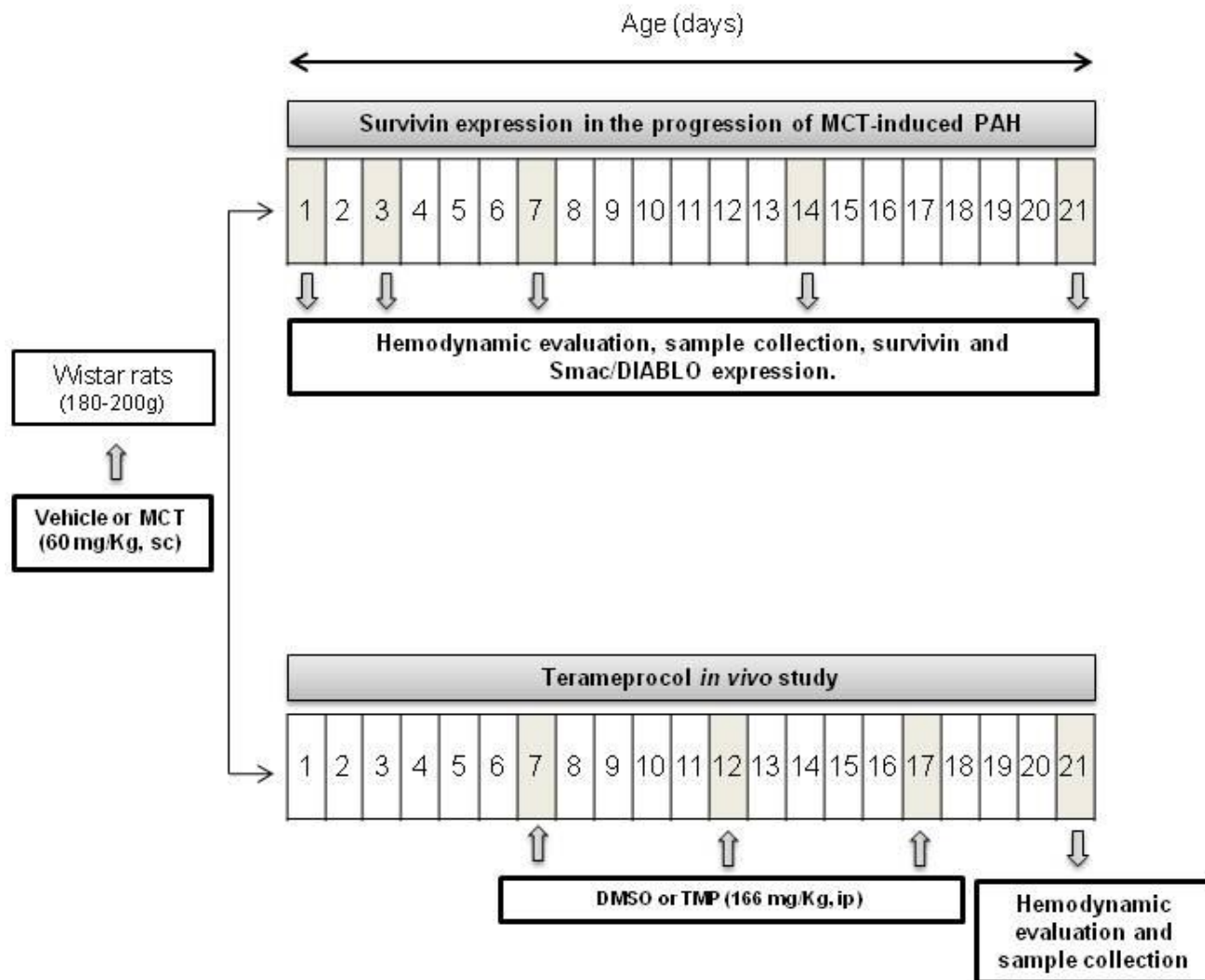


**Figure 4. Experimental design.** Progression of MCT-induced PAH and Terameprocol "in vivo" studies. MCT: Monocrotaline; PAH: Pulmonary arterial hypertension; sc: subcutaneous; DMSO: Dimethyl sulphoxide hybri-max; TMP: Terameprocol; ip: intraperitoneal.



### 3. Experimental Design

Animal experiments were performed according to the Portuguese law for animal welfare and conform to the National Institutes of Health Guide for the Care and Use of Laboratory Animals (NIH Pub. No. 85-23, Revised 2011). Figure 4. represents the studies performed.

#### 3.1. Survivin expression in the progression of MCT-induced PAH

Male Wistar Han rats (Charles River Laboratories, Barcelona, Spain) weighing 180-200 g were housed in groups of 5 animals/cage, in a controlled environment under a 12:12-h light-dark cycle at a room temperature of 22°C, with free supply of food and water. Rats randomly received a subcutaneous injection of MCT (60 mg/kg, Sigma, Barcelona, Spain) (MCT groups, n=15/time point) or an equal volume of vehicle (1 mL/kg of 0.9% NaCl) (SHAM groups, n=10/time point). In order to evaluate the progression of the disease, hemodynamic assessment was performed on days 1, 3, 7, 14 or 21 after MCT/vehicle injection followed by sample collection.

#### 3.2. Terameprocol in vivo study

Animals were randomly submitted to four different protocols: i) SHAM injected Dimethyl sulphoxide hybri-max (DMSO, 1 mL/Kg, intraperitoneal (ip); Sigma, Barcelona, Spain) (Sham+Vehicle, n=10), ii) SHAM injected with tetra-O-methyl nordihydroguaiaretic acid (Terameprocol or TMP, 166 mg/Kg, ip; Cayman Chemical, Michigan, USA) (Sham+TMP, n=10) iii) MCT injected with DMSO (MCT+Vehicle, n=15) and iv) MCT injected with TMP (MCT+TMP, n=15). DMSO or TMP were administrated at day seven after MCT or vehicle injection, a time point where significant morphological and molecular alterations were already noted in the first study, and at every five days until hemodynamic evaluation (21 days after MCT or vehicle).

### 4. Hemodynamic analysis

Animals were anesthetized by inhalation of mixture of sevoflurane (4%) and oxygen, intubated for mechanical ventilation (Dual Mode, Kent Scientific, Connecticut, USA) and placed over a heating pad (body temperature was maintained at 37°C). Under binocular surgical microscopy (Wild M651.MS-D, Leica; Herbrugg, Switzerland), the right jugular vein was cannulated for fluid administration (prewarmed 0.9% NaCl solution) to compensate for perioperative losses. The heart was exposed by a median sternotomy and the pericardium was widely opened. Bi-ventricular hemodynamic function was measured with pressure-volume (PV) catheters (PVR-1045 for RV and PVR-1035 for LV, Millar instruments, Houston, USA). Data was continually acquired (MPVS 300, Millar Instruments, Houston, USA) and digitally recorded at 1000Hz

(ML880 PowerLab 16/30, Millar TM instruments, Houston, USA). After complete instrumentation, the animal preparation was allowed to stabilize for 15 min. Hemodynamic recording was made under basal conditions and under vena cava, ascending aorta or pulmonary artery occlusion with respiration suspended at end-expiration. Parallel conductance values were obtained by the injection of approximately 100  $\mu$ l of 10% NaCl into the right atrium. Calibration from relative volume units (RVU) conductance signal to absolute volumes ( $\mu$ l) was undertaken using a previously validated method of comparison to known volumes in Perspex wells<sup>149</sup>. Heart rate (HR), RV and LV peak systolic pressure ( $P_{\max}$ ), end-diastolic pressure (EDP), peak rate for pressure rise ( $dP/dt_{\max}$ ), peak rate of pressure decline ( $dP/dt_{\min}$ ), constant time of isovolumetric pressure decline (Tau), ejection fraction (EF), cardiac output (CO) and maximal elastance (Ea) were obtained and analysed using PVAN 3.5 and LabChart 7.0 (Millar Instruments, Houston, USA).

## 5. Tissue Preparation

The heart (H), lungs and right *gastrocnemius* muscle were excised and weighted. The right tibia was also excised and its length was measured with a millimetric ruler. Under binocular magnification (x3.5, Wild M651.MS-D, Leica; Herbrugg, Switzerland), the RV free wall was dissected from the left ventricle + septum (S) and weighted separately. Heart, lungs, RV and LV+S weights were normalized to body weight (BW) and *gastrocnemius* weight was normalized to tibial length. Samples from heart and lung were fixed and included in paraffin for light microscopy, or frozen with liquid nitrogen for molecular studies.

## 6. Morphometric analysis

Samples of RV, LV (midway between the apex and base) and lung were fixed in 4% (v/v) buffered paraformaldehyde followed by dehydration with graded ethanol, diaphanization with xylene and included in paraffin blocks. Serial sections (4  $\mu$ m of thickness) of paraffin blocks were cut by a microtome (RM2125RTS, Leica, Nussloch, Germany) and mounted on silane-coated slides. The slides were dewaxed in xylene, hydrated through graded alcohols and stained for haematoxylin-eosin by immersing slides in Mayer's haematoxylin solution for 5 min. followed by immersion in aqueous eosin solution for 5 min. Slides were after submitted to graded alcohols and xylene and mounted with Entellan. Studied samples were observed at light microscopy (Dialux 20, Leitz, Wetzlar, Germany), photographed with a digital camera (XC30, Olympus, California, USA) and measured with a digital image analyzer (cell^B life science basic imaging software, Olympus, California, USA). Five images of random microscopic fields (magnification of x400) were obtained from each section to compensate for variations within sections. Only round to ovoid muscle fibers with a nuclear profile were counted to measure the cardiomyocytes surface area (CSA) being 500 cardiomyocytes/group/time point analyzed. On pulmonary specimens, external diameter and medial wall thickness in muscular arteries (20-25 arteries/animal, 10 animals/group/time point) were analyzed.

Orthogonal intercepts were used to generate eight random measurements of external diameter (distance between the external lamina) and sixteen random measurements of medial thickness (distance between the internal and external lamina). For each artery medial hypertrophy was expressed as follows: % wall thickness = [(medial thickness x 2) / (external diameter)] x 100.

## 7. Immunohistochemistry

Immunohistochemistry was performed to determine survivin and Smac/DIABLO expression in the RV. Sections (4 µm) were placed on SuperFrost®Plus slides followed by deparaffinization, rehydration, and subjected to heat induced antigen retrieval by immersion in 10 mM sodium citrate buffer (C<sub>6</sub>H<sub>5</sub>Na<sub>3</sub>O<sub>7</sub>·2H<sub>2</sub>O, pH 6.0) in the microwave for 30 min. Endogenous peroxidase activity was blocked by 3% hydrogen peroxide for 10 min. at room temperature (RT). Blockage of non-specific binding was performed with 5% normal goat serum (NGS) in TBS (100 mM Tris, 1.5 mM NaCl, pH 8.0) 0.1% Tween-20 (TBS-T) for 1 hour, RT flowed by 3 washes, 5 min. each in TBS-T. Sections were encircled with a pap pen (Vector Laboratories, California, USA) to prevent splitting leakage of the flowing incubation solutions. Endogenous avidin-biotin expression was blocked using an endogenous avidin + biotin blocking system, (ab3387, abcam, Cambridge, UK), according to manufacturer's instructions, being followed by incubation with the primary antibodies (1:500 dilution; rabbit anti-survivin, ab469; dilution 1:250; rabbit anti-Smac/DIABLO, ab8115, abcam, Cambridge, UK) overnight at 4°C. After incubation with primary antibodies, slides were washed 3 times, 5 min each with TBS-T, RT and incubated with goat anti-rabbit IgG secondary antibody (1:250 dilution; ab6720, abcam, Cambridge, UK) for 2 hours, RT. Slides were submitted to another 3 washes, 5min each in TBS-T, RT prior being incubated with streptavidin protein, HRP (1:1000 dilution; ab7403, abcam, Cambridge, UK). To visualize the peroxidase activity in sections 3,3-diaminobenzidine (DAB, ab94665, abcam, Cambridge, UK) was used. Finally, slides were counterstained with Mayer's haematoxylin, submitted to graded alcohols and xylene and mounted with Entellan. Negative control reactions included omission of the primary antibody. The slides were observed and photographed with a microscope (Dialux 20, Leitz, Wetzlar, Germany) under x400 magnification. Survivin and Smac/DIABLO expression was qualitatively determined as positive (cytoplasmatic staining) or negative (500 cardiomyocytes/group/time point).

## 8. Western Blotting

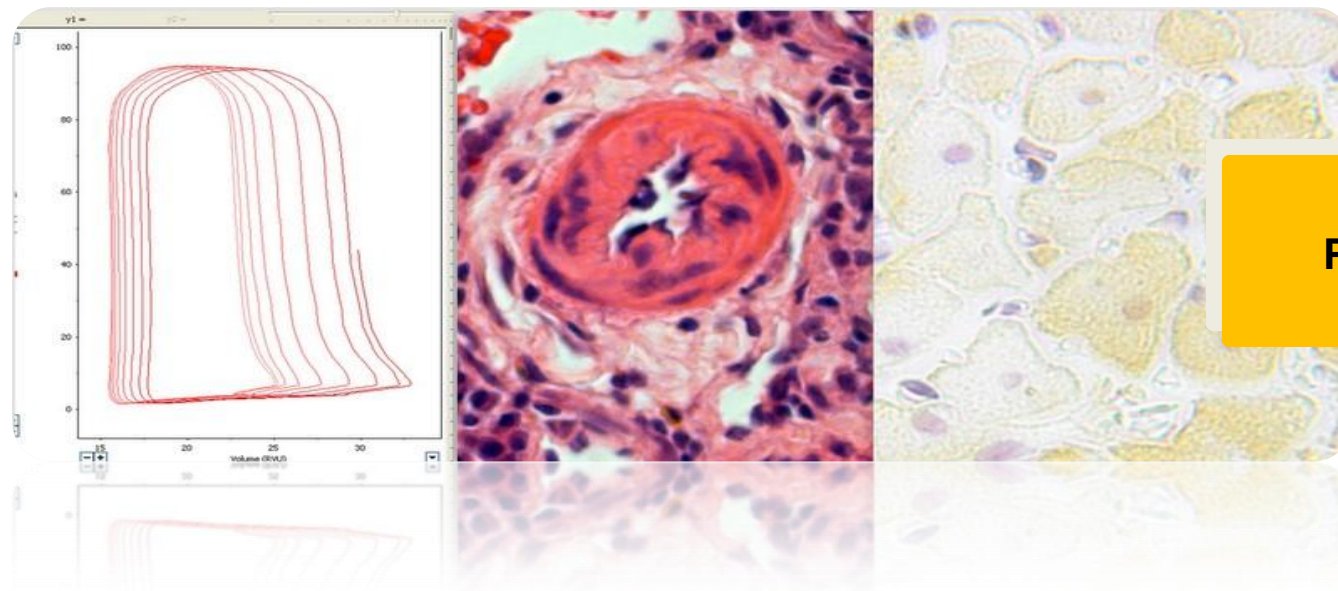
RV, LV and lung samples (n=6 animals/group/time point) previously frozen with liquid nitrogen were homogenised in phosphate buffer (13 mM KH<sub>2</sub>PO<sub>4</sub>, 54mM NaHPO<sub>4</sub>, pH 7.4) (in the proportion of 1:20) with a Bio-Gen PRO200 homogeniser (Pro 200, Pro Scientific, Connecticut, USA). Total protein concentration was spectrophotometrically determined with the colorimetric method RC-DC protein assay (Bio-Rad,

California, USA). The optic density was determined at 750nm in a microplate reader (UVM340, Asys, Cambridge, UK). Simultaneously, a calibration curve was performed using different concentrations of bovine serum albumin (BSA).

Equivalent amounts of total protein from the homogenized RV, LV and lung of each group were electrophoresed on a 12.5% SDS-PAGE at 200V at room temperature as described by Laemmli<sup>150</sup>. Gels containing total proteins were transferred to a nitrocellulose membrane (0.2 µm, Bio-Rad, California, USA) in 25 mM Tris, 192 mM and 20% methanol at 200 mA. Equal loading of membranes was confirmed by staining the membranes with Ponceau S and nonspecific binding was blocked with 5 % (w/v) dry non-fat milk in TBS-T. Membranes were incubated with primary antibody (1:1000 dilution; rabbit anti-survivin, ab469; 1:500 dilution, rabbit anti-Smac/DIABLO, ab8115, abcam, Cambridge, UK) overnight at 4°C with agitation. Afterwards, blots were washed in TBS-T and incubated with a secondary antibody (1:15000, LI-COR IRDye® 800CW, Nebraska, USA). Immunoreactive bands were observed under fluorescence using an Odyssey system (LI-COR Odyssey, Nebraska, USA) and the results were analyzed with Quantity One software v. 4.6.3 (Bio-Rad, California, USA).

## 9. Statistical Analysis

Statistical analysis was performed using Graph Pad Prism software (version 5.0, Graph Pad software, California, USA). All data are presented as mean ± SEM and were compared using Two Way ANOVA. When treatments were significantly different, Students-Newman Keuls post-hoc test was selected to perform pairwise multiple comparisons. Results were considered significantly different when  $p < 0.05$ .



## Part IV – Results

## 10. Progression of MCT-induced pulmonary arterial hypertension

### 10.1. Right ventricle hemodynamic evaluation

Table 4. represents the results from RV hemodynamic evaluation. RVPmax, dP/dtmax and dP/dtmin were significantly different between Sham and MCT groups 14 and 21 days after injection. Also, in MCT groups and at day 21, RVPmax was significantly augmented when compared with the previous time-points. MCT treatment did not induce any alterations in heart rate and end-diastolic pressure.

### 10.2. Morphometric analysis

Table 5. summarizes the morphometric progression of MCT-induced PAH. In Sham groups there is a significant increase in body weight throughout the protocol. In contrast, MCT animals had a lower weight gain being significantly different at day 21 after injection. No variation in the relation HT/BW was observed in MCT group, while it was reduced in the Sham group on days 14 and 21. MCT administration induced hypertrophy as expressed by the indexes RV/(LV+S) and RV/BW, both significantly increased on D21. Also, MCT-treated animals developed hypertrophy at cellular level represented by a significant increase in RV cardiomyocyte cross sectional area since day 7 after injection and progressively until day 21. Neither groups presented any changes in the left ventricle ((LV+S)/BW parameter).

**Table 3.** Right ventricle hemodynamic evaluation parameters.

	D1		D3		D7		D14		D21	
	Sham	MCT	Sham	MCT	Sham	MCT	Sham	MCT	Sham	MCT
Heart rate (bpm)	378 ± 23	413 ± 14	410 ± 18	387 ± 20	349 ± 22	357 ± 10	358 ± 35	385 ± 30	340 ± 14	376 ± 23
P <sub>max</sub> (mmHg)	28.0 ± 1.9	28.3 ± 2.1	27.2 ± 0.8	28.2 ± 1.6	27.3 ± 2.2	31.5 ± 1.5	23.7 ± 1.0	31.9 ± 1.3 *	26.3 ± 1.2	38.9 ± 2.7 <sup>*,a,b,c,d</sup>
EDP (mmHg)	3.9 ± 0.5	2.7 ± 0.3	3.2 ± 0.3	2.7 ± 0.3	3.9 ± 0.3	4.2 ± 1.0	3.9 ± 0.2	3.4 ± 0.7	3.6 ± 0.4	3.5 ± 0.3
dP/dt <sub>max</sub> (mmHg/sec)	1671 ± 152	1858 ± 184	1901 ± 90	2102 ± 217	1685 ± 155	1906 ± 83	1405 ± 101	2233 ± 190 *	1563 ± 60	2257 ± 65 *
dP/dt <sub>min</sub> (mmHg/sec)	-1544 ± 355	-1421 ± 189	-1629 ± 109	-1702 ± 230	-1624 ± 204	-1441 ± 142	-1020 ± 144	-1830 ± 172 *	-1228 ± 113	2263 ± 93 <sup>*,b,c</sup>

P<sub>max</sub>: maximum pressure; EDP: end-diastolic pressure; dP/dt<sub>max</sub>: peak rate of pressure rise; dP/dt<sub>min</sub>: peak rate of pressure fall. Data are mean±SEM. Sham: sham group; MCT: monocrotaline group. \*p < 0.05 vs. Sham of the same day; <sup>a</sup>p < 0.05 vs. D14 of the same treatment group, <sup>b</sup>p < 0.05 vs. D7 of the same treatment group; <sup>c</sup>p < 0.05 vs. D3 of the same treatment group; <sup>d</sup>p < 0.05 vs. D1 of the same treatment group.

**Table 4.** Morphometric progression of MCT-induced PAH.

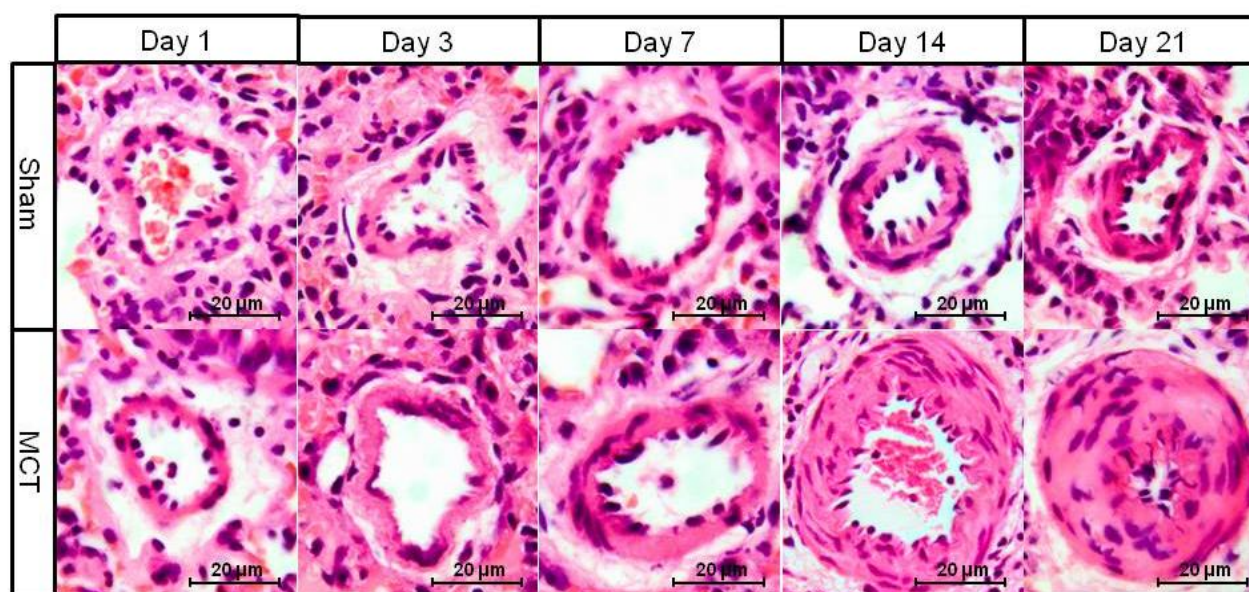
	D1		D3		D7		D14		D21	
	Sham	MCT	Sham	MCT	Sham	MCT	Sham	MCT	Sham	MCT
Body weight (g)	194.1 ± 5.1	195.4 ± 5.9	211.0 ± 4.7 <sup>d</sup>	198.6 ± 1.7	230.4 ± 8.2 <sup>c,d</sup>	214.6 ± 3.2	262.2 ± 9.5 <sup>b,c,d</sup>	253.7 ± 6.0 <sup>b,c,d</sup>	290.6 ± 4.5 <sup>a,b,c,d</sup>	260.8 ± 4.9 <sup>*,b,c,d</sup>
HW/BW (g/Kg)	3.271 ± 0.028	3.243 ± 0.091	3.242 ± 0.047	3.189 ± 0.059	3.031 ± 0.079	3.129 ± 0.061	2.862 ± 0.037 <sup>c,d</sup>	3.025 ± 0.051	2.794 ± 0.069 <sup>c,d</sup>	3.282 ± 0.113 <sup>*</sup>
RV/(LV+S) (g/g)	0.264 ± 0.014	0.265 ± 0.021	0.268 ± 0.013	0.260 ± 0.005	0.282 ± 0.017	0.332 ± 0.021	0.287 ± 0.018	0.320 ± 0.011	0.302 ± 0.012	0.467 ± 0.049 <sup>*,a,b,c,d</sup>
RV/BW (g/Kg)	0.578 ± 0.025	0.591 ± 0.040	0.578 ± 0.023	0.590 ± 0.016	0.583 ± 0.038	0.665 ± 0.036	0.560 ± 0.032	0.608 ± 0.021	0.584 ± 0.013	0.911 ± 0.095 <sup>*,a,b,c,d</sup>
(LV +S)/BW (g/Kg)	2.197 ± 0.037	2.240 ± 0.037	2.165 ± 0.030	2.274 ± 0.061	2.070 ± 0.058	2.011 ± 0.047 <sup>c,d</sup>	1.956 ± 0.037 <sup>c,d</sup>	1.900 ± 0.026 <sup>c,d</sup>	1.957 ± 0.060 <sup>c,d</sup>	1.956 ± 0.042 <sup>c,d</sup>
RV CSA (µm²)	131.2 ± 2.4	134.1 ± 1.9	128.2 ± 2.3	132.4 ± 2.2	139.6 ± 2.4	151.5 ± 2.6 <sup>*,c,d</sup>	197.9 ± 5.2 <sup>b,c,d</sup>	254.0 ± 6.0 <sup>*,b,c,d</sup>	169.5 ± 4.4 <sup>a,b,c,d</sup>	332.8 ± 10.0 <sup>*,a,b,c,d</sup>
L/BW (g/Kg)	5.731 ± 0.260	5.592 ± 0.117	5.426 ± 0.202	5.311 ± 0.140	5.436 ± 0.307	5.896 ± 0.400	4.661 ± 0.173	5.639 ± 0.220 <sup>*</sup>	4.782 ± 0.323	7.241 ± 0.464 <sup>*,a,b,c,d</sup>
G/Tib (g/cm)	0.341 ± 0.008	0.337 ± 0.023	0.348 ± 0.008	0.345 ± 0.012	0.382 ± 0.012	0.374 ± 0.004	0.423 ± 0.020	0.416 ± 0.013	0.440 ± 0.016	0.430 ± 0.008

HW/BW: heart weight/body weight; RV/(LV+S): right ventricle/(left ventricle+septum); RV/BW: right ventricle/body weight; (LV+S)/BW: (left ventricle+septum)/body weight; CSA: cross sectional area; L/BW: lung/body weight; G/Tib: gastrocnemius/tibia; Sham: sham group; MCT: monocrotaline group Data are mean±SEM. <sup>\*</sup>p < 0.05 vs. Sham of the same day; <sup>a</sup>p < 0.05 vs. D14 of the same treatment group, <sup>b</sup>p < 0.05 vs. D7 of the same treatment group; <sup>c</sup>p < 0.05 vs. D3 of the same treatment group; <sup>d</sup>p < 0.05 vs. D1 of the same treatment group.



Normalized lung weight was significantly increased in MCT groups compared with Sham groups in days 14 and 21. Also in MCT treated animals, at D21, the L/BW parameter was significantly higher when compared to the other time-points evaluated. As demonstrated in Figure 5. pulmonary arterial wall suffered a significant thickening from day 14 and forward in MCT groups.

**A**



**B**

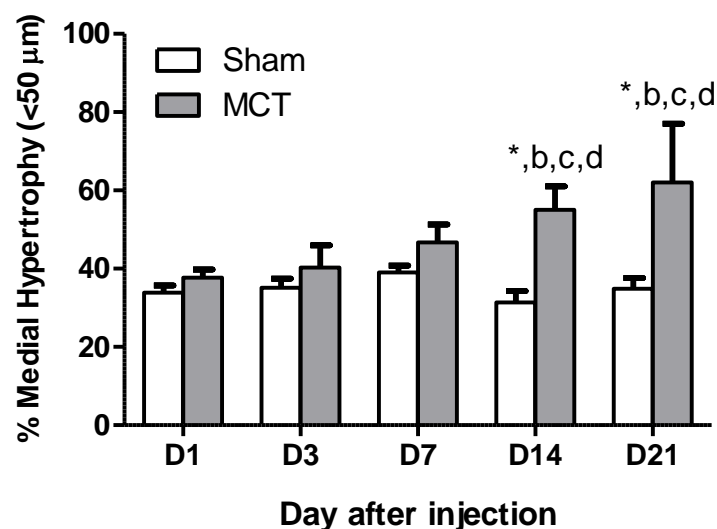


**Figure 5. Pulmonary arterial hypertrophy.** A) Histological appearance of small pulmonary arteries stained with hematoxylin and eosin; B) Percentage of arterial medial layer hypertrophy. Sham: Sham group; MCT: monocrotaline group. Data are mean±SEM; \*p < 0.05 vs. Sham of the same day, <sup>b</sup>p < 0.05 vs. D7 of the same treatment group, <sup>c</sup>p < 0.05 vs. D3 of the same treatment group, <sup>d</sup>p < 0.05 vs. D1 of the same treatment group.

### 10.3. Survivin and Smac/DIABLO expression

Lung survivin and Smac/DIABLO expression are shown in Figures 6, A and B. Survivin expression is augmented in MCT groups in days 7 and 21 when compared with Sham groups. Moreover, MCT groups presented a significant reduction from day 7 to day 21. No differences were noted between days in Sham groups. In contrast, pulmonary Smac/DIABLO expression decreases in MCT groups compared to Sham groups in both time-points.

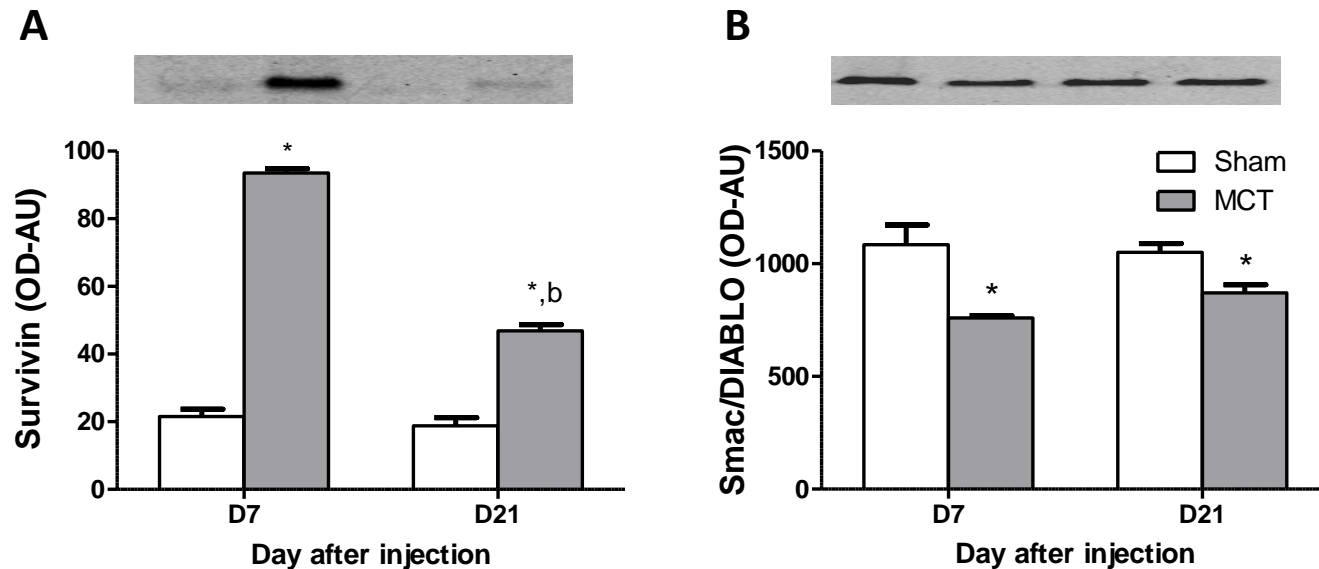


**Figure 6. Pulmonary survivin and Smac/DIABLO expression (A and B, respectively),** evaluated by western blot. Sham: sham group, MCT: monocrotaline group. Data are mean $\pm$ SEM. \* $p < 0.05$  vs. Sham of the same day, <sup>b</sup> $p < 0.05$  vs. D7 of the same treatment group.

Figure 7. (A, B and C) shows survivin expression in the right ventricle. When in comparison with Sham group, MCT treated animals survivin expression is barely present on day 3 after injection and significantly rises on day 7, further increasing throughout days 14 and 21. Confirmation by western blotting (C) demonstrated a significantly increase in protein expression in MCT groups between day 7 and 21 after injection. Sham groups do not suffer any alteration between time points. Contrarily, MCT groups presented a lower Smac/DIABLO expression since D3 and forward when compared with Sham animals. (Figure 8. A, B and C)

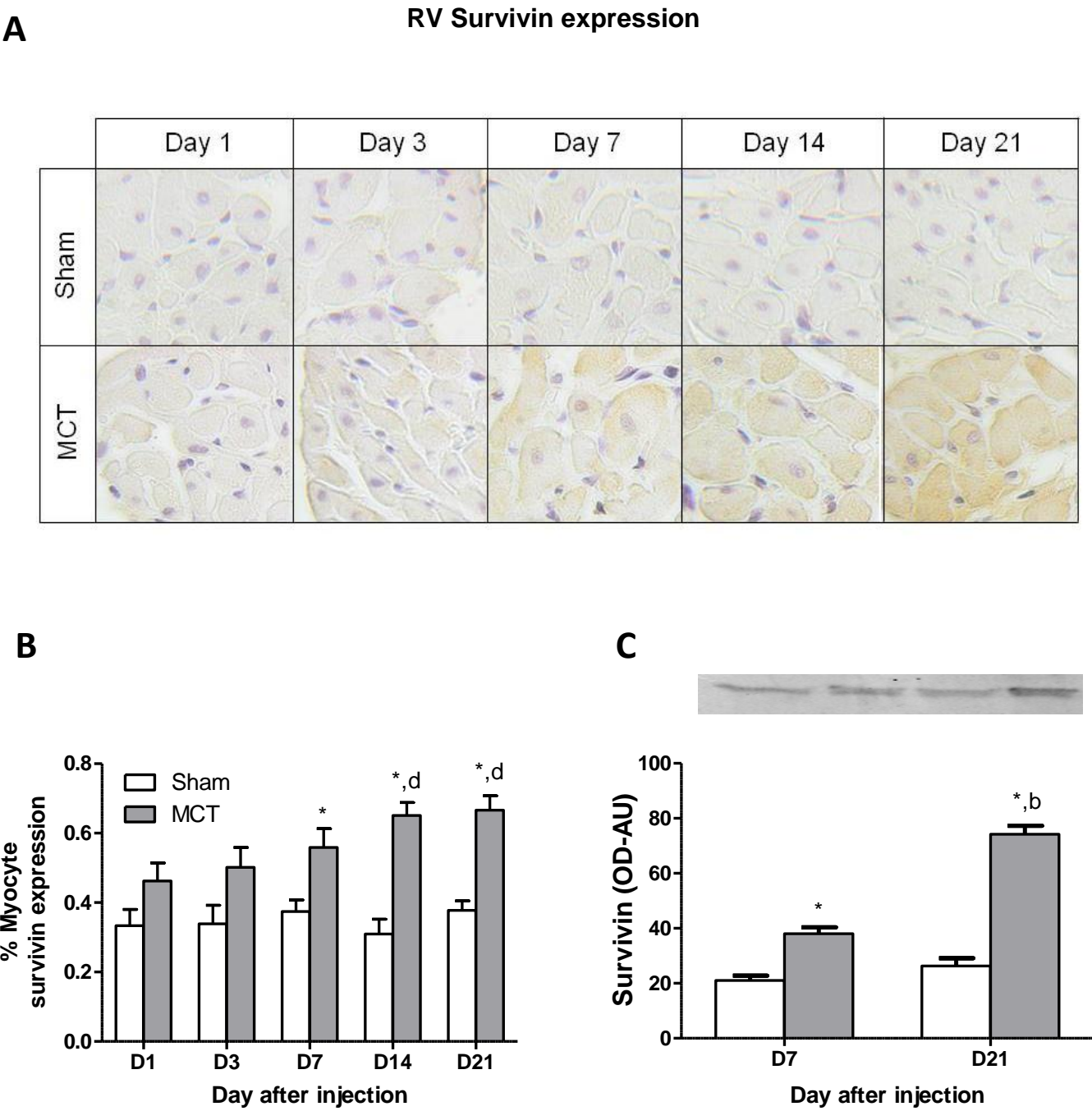


**Figure 7. Survivin expression in the right ventricle** evaluated by immunohistochemistry (A and B) and by western blot (C) during the progression of pulmonary arterial hypertension. Sham: Sham group, MCT: monocrotaline group. Data are mean±SEM. \*p < 0.05 vs. Sham of the same day, <sup>b</sup>p < 0.05 vs. D7 of the same treatment group, <sup>d</sup>p < 0.05 vs. D1 of the same treatment group.

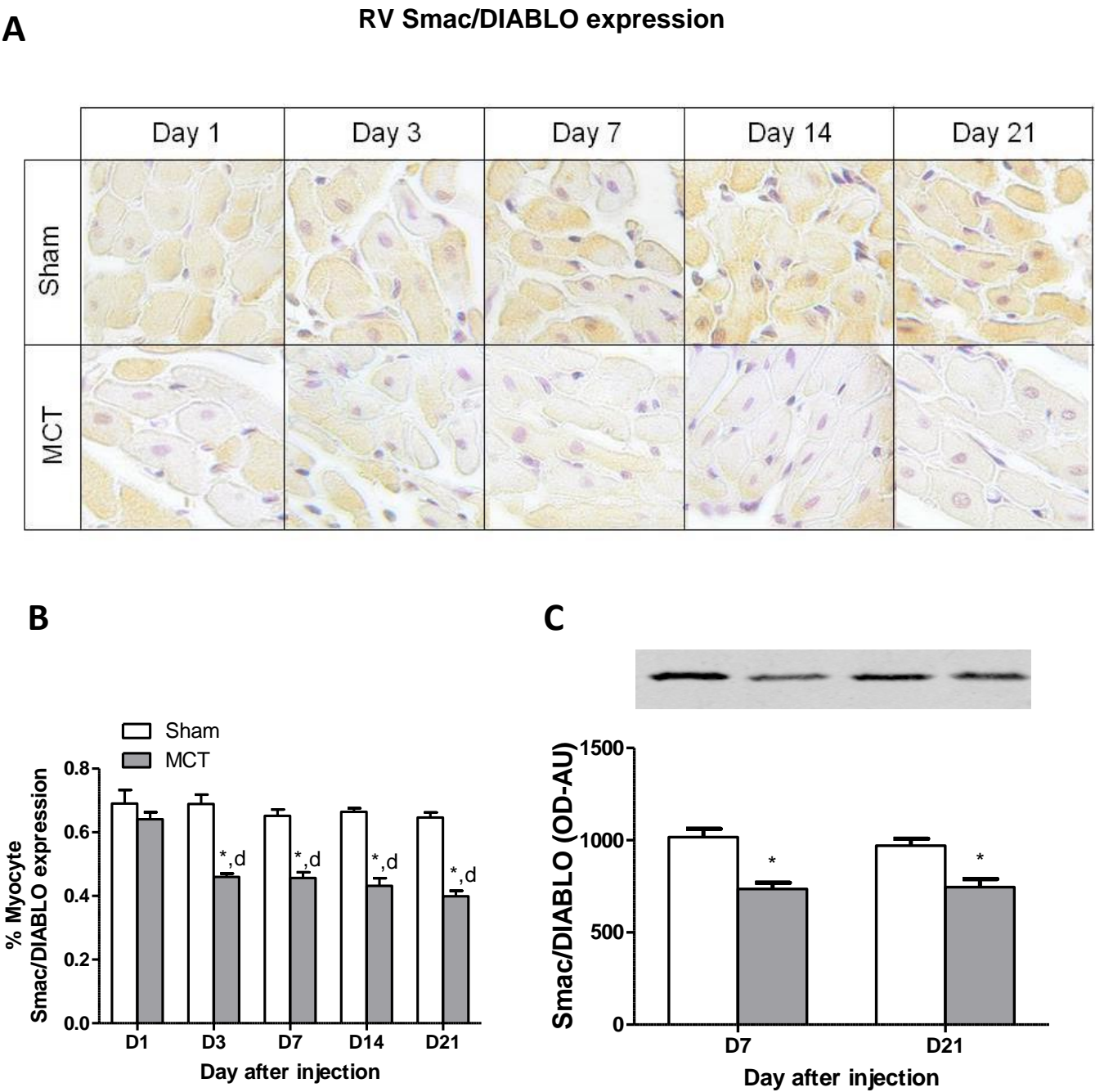


**Figure 8. Smac/DIABLO expression in the right ventricle** evaluated by immunohistochemistry (A and B) and by western blot (C) during the progression of pulmonary arterial hypertension. Sham: Sham group, MCT: monocrotaline group. Data are mean±SEM. \*p < 0.05 vs. Sham of the same day, <sup>d</sup>p < 0.05 vs. D1 of the same treatment group.

## 11. Terameprocol *in vivo* study

### 11.1. Regression of RV dysfunction in MCT animals treated with TMP

Table 6. summarizes the results from bi-ventricular hemodynamic evaluation. In MCT+TMP animals, TMP treatment reverted the augmentation in  $RVP_{max}$  observed in MCT+Vehicle group (Figure 9. A). Inversely, CO was diminished in MCT+Vehicle animals and chronic TMP administration returned this parameter back to its normal condition (Figure 9. B). No alterations were noted in Sham groups.

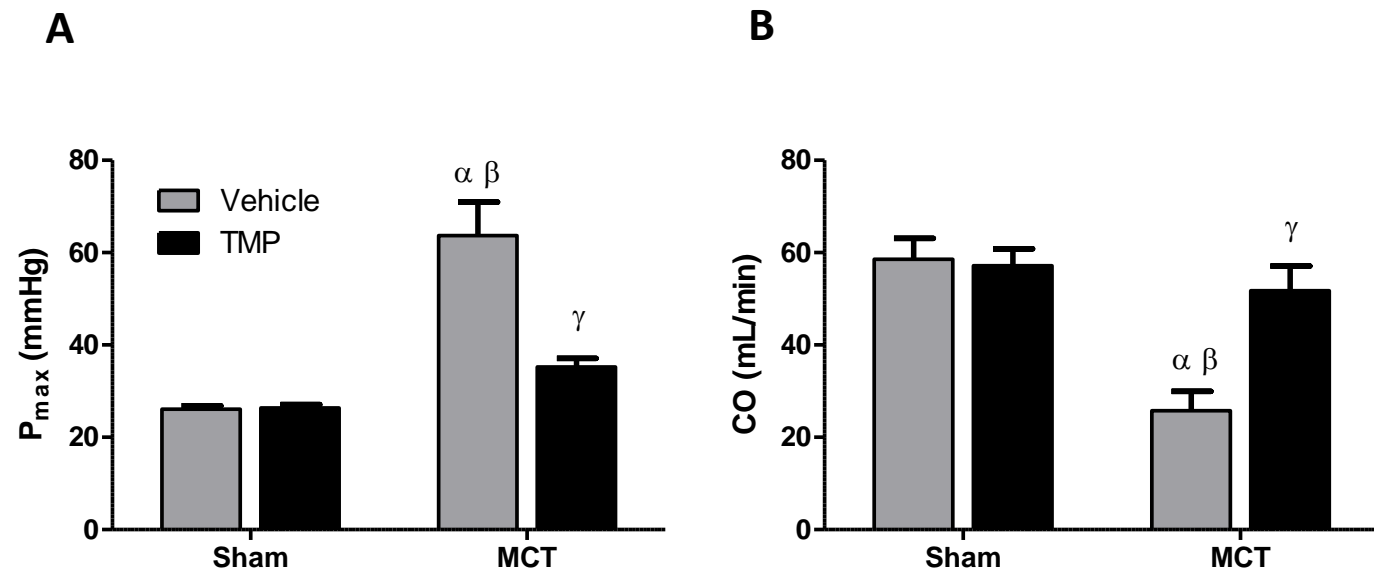


**Figure 9. Terameprocol effects on RV maximal pressure and cardiac output (A and B, respectively).** Sham: Sham group, MCT: monocrotaline group, TMP: Terameprocol, CO: cardiac output,  $P_{max}$ : maximum pressure. Data are mean±SEM.  $\alpha$ p < 0.05 vs. Sham+V,  $\beta$ p < 0.05 vs. Sham+TMP and  $\gamma$ p < 0.05 vs. MCT+V.

Peak rates of RV pressure rise and fall as well as Ea and EF were increased in MCT groups treated with vehicle. In MCT+TMP animals the increase was significantly reduced.

Diastolic function was markedly impaired in MCT+Vehicle group, namely there was an increase in end-diastolic pressure and a longer RV time constant tau. TMP injections normalized both end-diastolic pressure and tau in MCT treated animals.

Regarding the left ventricle assessment no significant alterations were registered.



**Table 5.** Terameprocol effects on cardiac hemodynamics

	Sham		MCT	
	Vehicle	TMP	Vehicle	TMP
Heart rate (bpm)	380.5 ± 8.402	376.5 ± 8.425	365.4 ± 5.608	386.1 ± 7.373
<b>RV Function</b>				
dP/dt <sub>max</sub> (mmHg/sec)	1500 ± 26.55	1627 ± 65.47	3450 ± 468.6 <sup>α β</sup>	2107 ± 83.22 <sup>γ</sup>
dP/dt <sub>min</sub> (mmHg/sec)	-1485 ± 151.4	-1325 ± 18.62	-2903 ± 165.4 <sup>α β</sup>	-1763 ± 27.86 <sup>β γ</sup>
EF (%)	65.42 ± 5.536	70.04 ± 3.858	29.41 ± 4.383 <sup>α β</sup>	70.56 ± 4.902 <sup>γ</sup>
EDP (mmHg)	2.951 ± 0.1836	3.561 ± 0.4696	6.424 ± 1.137 <sup>α β</sup>	3.165 ± 0.6209 <sup>γ</sup>
Ea (mmHg/μL)	0.1528 ± 0.0115	0.1468 ± 0.0079	0.7701 ± 0.1588 <sup>α β</sup>	0.2661 ± 0.0372
Tau (ms)	10.84 ± 0.7640	10.43 ± 0.7636	15.96 ± 0.3210 <sup>α β</sup>	9.229 ± 0.7491 <sup>γ</sup>
<b>LV Function</b>				
P <sub>max</sub> (mmHg)	84.89 ± 5.706	94.14 ± 1.525	97.17 ± 4.977	94.66 ± 3.743
dP/dt <sub>max</sub> (mmHg/sec)	5582 ± 460.5	6517 ± 297.9	5724 ± 217.8	5518 ± 321.0
dP/dt <sub>min</sub> (mmHg/sec)	-5180 ± 888.4	-6785 ± 430.0	-5242 ± 458.3	-6434 ± 380.8
EF (%)	73.82 ± 3.931	72.89 ± 4.410	71.47 ± 2.945	68.72 ± 3.969
EDP (mmHg)	5.427 ± 1.538	4.376 ± 1.272	4.531 ± 0.7069	6.576 ± 1.885
Ea (mmHg/μL)	0.4007 ± 0.076	0.4911 ± 0.0645	0.7408 ± 0.1039	0.7330 ± 0.1712
Tau (ms)	8.609 ± 0.3356	9.136 ± 0.8681	9.015 ± 0.5702	9.754 ± 0.6173

Sham: Sham group, MCT: monocrotaline group. TMP: Terameprocol; P<sub>max</sub>: maximum pressure; dP/dt<sub>max</sub>: peak rate of pressure rise; dP/dt<sub>min</sub>: peak rate of pressure fall; EF: Ejection fraction; EDP: end-diastolic pressure; Ea: arterial elastance; Tau: time constant of ventricular decay. Data are mean±SEM. <sup>α</sup>p < 0.05 vs. Sham+V, <sup>β</sup>p < 0.05 vs. Sham+TMP and <sup>γ</sup>p<0.05 vs. MCT+V.

## 11.2. Terameprocol reverts pulmonary and cardiovascular remodelling

A lower body weight was observed in both MCT groups (Table 7.). MCT injection induced an increase in heart weight (HW) in MCT+V animals that was reverted with the injection of TMP as shown by HW/BW ratio (Table 7.). Moreover, MCT and TMP administration did not induced any alterations in LV morphometric parameters. Regarding Sham groups there were no differences in right or left ventricle parameters.

**Table 6.** Effects of Terameprocol in morphometric characteristics.

	Sham		MCT	
	Vehicle	TMP	Vehicle	TMP
Body weight (g)	300.1 ± 8.2	268.6 ± 11.4	258.6 ± 5.6 <sup>α</sup>	249.7 ± 8.0 <sup>α</sup>
HW/BW (g/Kg)	3.013 ± 0.103	2.734 ± 0.096	3.634 ± 0.317 <sup>α,β</sup>	3.068 ± 0.176 <sup>γ</sup>
RV/(LV+S) (g/g)	0.3043 ± 0.0109	0.3401 ± 0.0299	0.4589 ± 0.0362 <sup>α,β</sup>	0.3685 ± 0.0189 <sup>γ</sup>
(LV+S) /BW (g/Kg)	1.856 ± 0.052	1.771 ± 0.063	2.035 ± 0.081	1.837 ± 0.044
G/Tib (g/cm)	0.5200 ± 0.0147	0.4857 ± 0.0092	0.4951 ± 0.0138	0.4290 ± 0.0177

HW/BW: heart weight/body weight; RV/(LV+S): right ventricle/(left ventricle+septum); (LV+S)/BW: (left ventricle+Septum)/body weight; G/Tib: gastrocnemius/tibia. Sham: sham group; MCT: monocrotaline group; TMP: Terameprocol. Data are mean±SEM. <sup>α</sup>p < 0.05 vs. Sham+Vehicle; <sup>β</sup>p < 0.05 vs. Sham+TMP, <sup>γ</sup>p < 0.05 vs. MCT+Vehicle.

MCT induced RV hypertrophy in MCT animals injected with vehicle which was reverted by TMP as shown by RV/BW (Figure 10. A). This result was confirmed by histology where MCT administration induced hypertrophy at cardiomyocyte level. MCT+TMP exhibited significant less hypertrophy when compared with the other MCT animals (Figure 10. B).

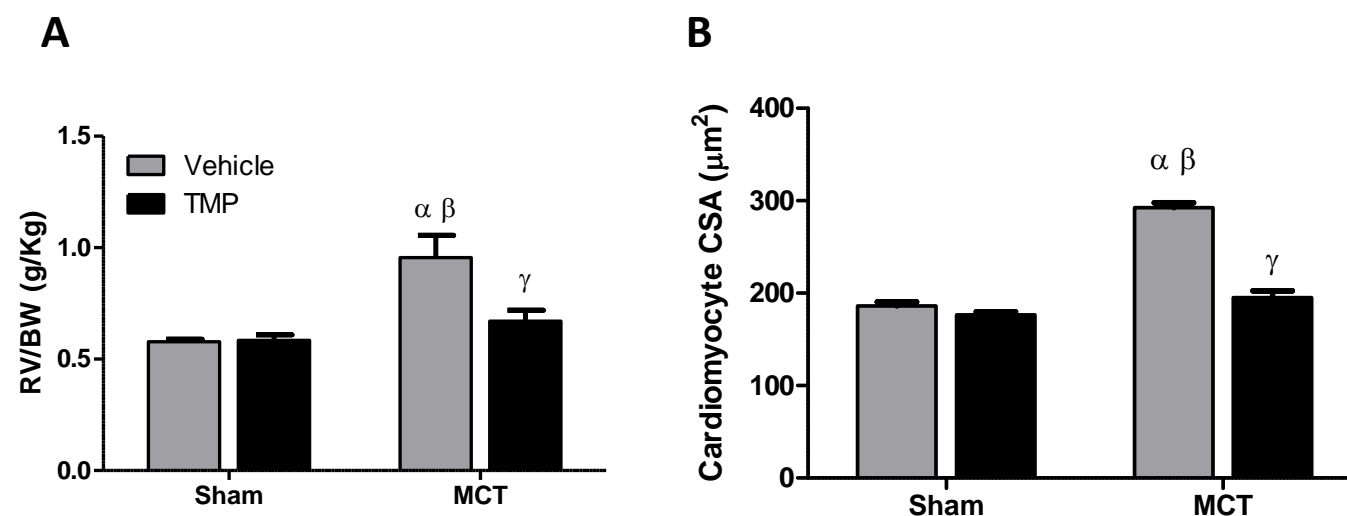
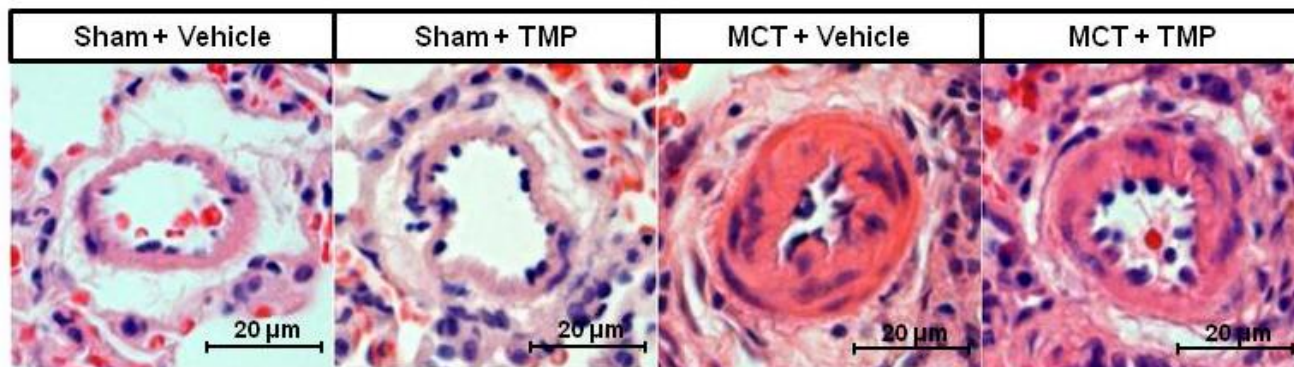


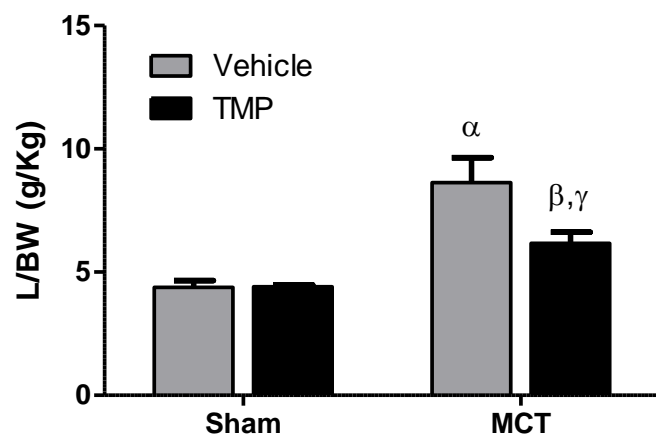
**Figure 10.** Terameprocol effects on the right ventricle structure demonstrated by right ventricle/body weight ratio (RV/BW) and cardiomyocyte cross sectional area (CSA) (A and B respectively). Sham: Sham group, MCT: monocrotaline group, TMP: Terameprocol. Data are mean±SEM. <sup>α</sup>p < 0.05 vs. Sham+V, <sup>β</sup>p < 0.05 vs. Sham+TMP and <sup>γ</sup>p<0.05 vs. MCT+V.

Regarding lung weight this was significantly increased in MCT+Vehicle as demonstrated by L/BW ratio. TMP injection reverted this parameter as well as attenuated the medial hypertrophy of the lung small caliber arteries when compared with MCT+Vehicle (Figure 11. A and C). No significant differences were noted in Sham groups.

A



B



C

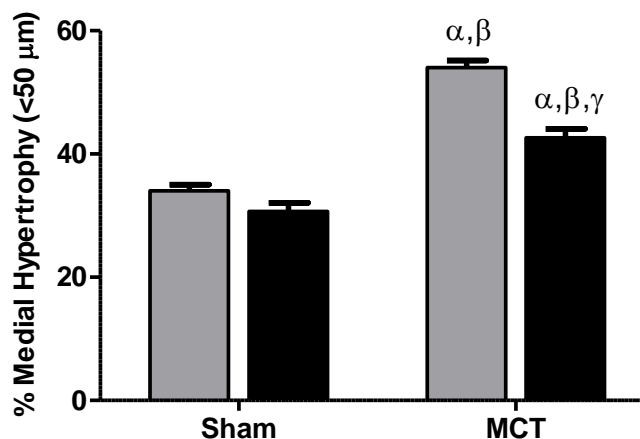
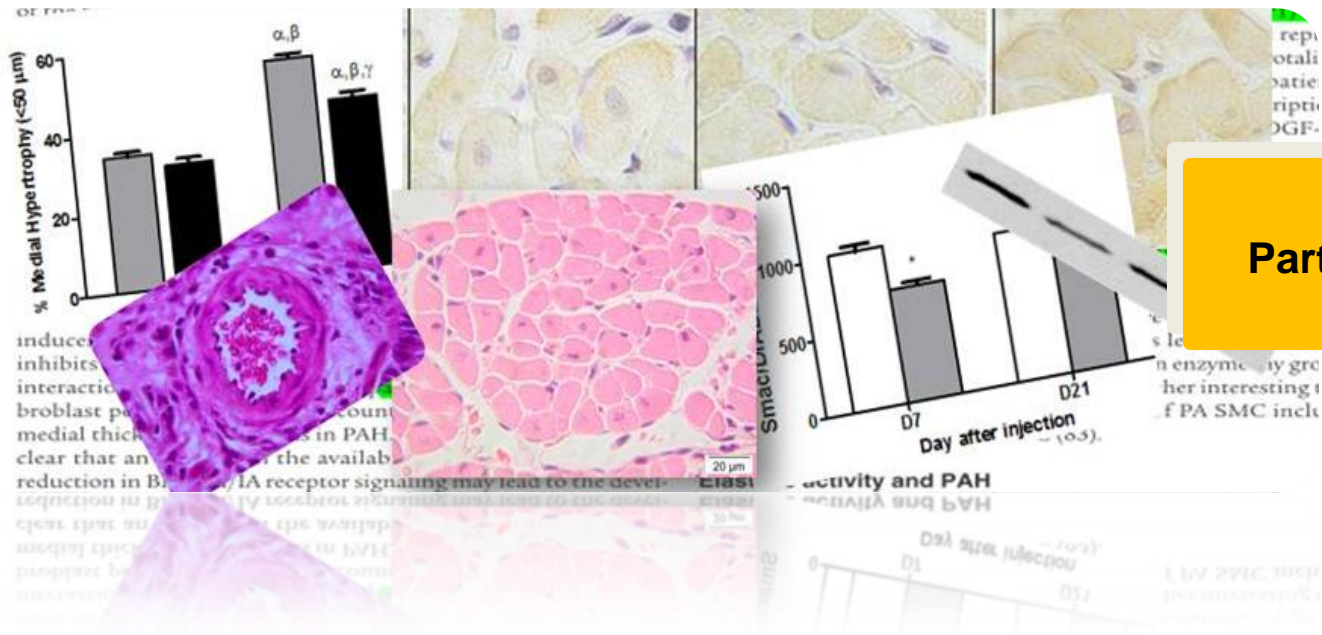


**Figure 11. Pulmonary response to Terameprocol** evaluated by lung weight/body weight ratio (L/BW) and by the percentage of medial hypertrophy of pulmonary arteries (B, A and C respectively). Sham: Sham group, MCT: monocrotaline group, TMP: Terameprocol. Data are mean±SEM. <sup>α</sup>p < 0.05 vs. Sham+V, <sup>β</sup>p < 0.05 vs. Sham+TMP and <sup>γ</sup>p<0.05 vs. MCT+V.





## Part V – Discussion

PAH is a multifactorial disorder that commonly leads to right heart failure and death. Throughout the years, research has been focusing on the rat model of MCT-induced PAH to better understand the disease as well as different therapeutic options. Even though alterations like plexiform lesions (typical in human disease) are not mimicked by this model, MCT induces pulmonary vascular remodeling and RV hypertrophy, both aims of our progression study. Moreover, most studies reflect the advanced stages of this pathology (D25-35 after MCT injection) probably because nearly all patients with PAH present with late-stage disease. To our knowledge studies on the early features of PAH are essential to better understand its development and pathophysiologic pathways. Current therapeutic options specifically focus on vasodilators, though with a very limited impact in the overall outcome of the patient. Therefore, research is pursuing strategies to reverse the remodeling of the pulmonary vasculatures by interfering with the disturbed balance between cell apoptosis and proliferation<sup>151, 152</sup>. In the present study we investigated the natural progression of MCT-induced PAH and identified the timing of appearance of its hemodynamic and morphological features correlated with apoptosis proteins: survivin and Smac/DIABLO expression. After establishing these proteins patterns we modulated it through chronic in vivo administration of terameprocol.

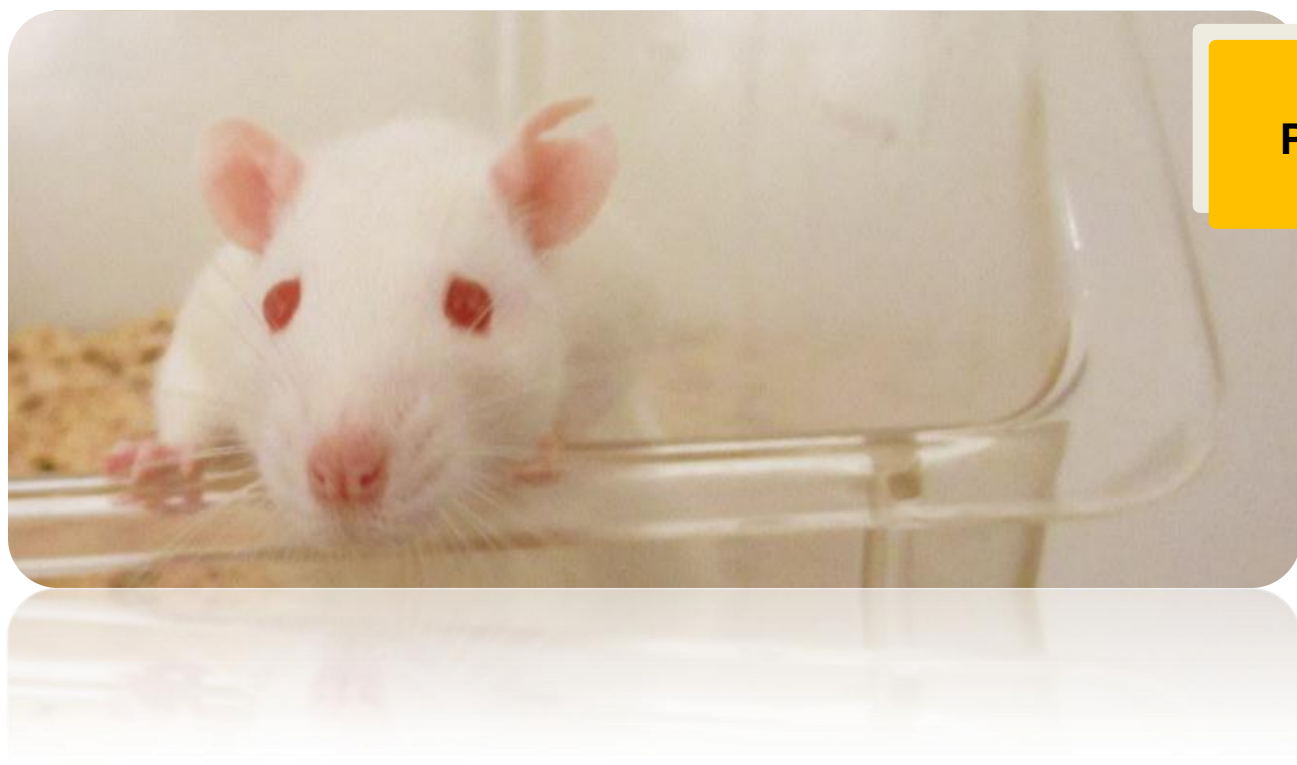
Survivin, an anti-apoptotic protein, has been reported to be significantly increased to aberrantly promote cell survival in neoplasia of various cancers<sup>111, 153</sup> being of interest also in PAH for the same reasons. In PAH, cardiac hypertrophy allows RV to endure the pressure overload in a compensatory response. The exact role of apoptosis and specially survivin in cardiovascular physiology and diseases still requires more research. Some groups demonstrated the cardioprotective increased expression of survivin in myocardial injury inversely correlated with apoptosis<sup>154-156</sup>. In fact, a study in a model of spontaneously hypertensive rats discovered that myocardial expression of survivin in ageing and HF is inversely correlated with cardiac apoptosis and associated with a more favorable cardiac remodeling<sup>156</sup>. Levkau and colleagues<sup>157</sup> also suggest a role of survivin in cardiac by showing it to be essential for the regulation of cardiomyocyte proliferation and mitosis. In fact, knockouts for survivin gene presented an inverse correlation between cardiomyocyte polyploidy and cardiomyocyte number leading to progressive HF and death. The same study demonstrated that survivin overexpression in cultured rat neonatal cardiomyocytes promoted cell division to protect those cells against apoptosis. Finally, Levkau established that only very low levels of survivin were present in normal human heart whereas patients with terminal HF showed increased levels of this anti-apoptotic protein. In the same patients, the expression of survivin was reverted after hemodynamic support through left ventricle assisting device (LVAD) raising the possibility that cardiac survivin expression is load-dependent. Supporting Levkau's hypothesis, in our study we demonstrated that survivin expression was progressively increased throughout the development of MCT-induced PAH. The first incidence of survivin augmentation was 7 days after MCT injection, the time point where RV cardiomyocyte hypertrophy is first present and where no hemodynamic dysfunction was noticed. Interestingly, RV hemodynamic alterations were only observed 14 days after MCT administration. Moreover, McMurtry and colleagues also demonstrated that lung survivin overexpression preceded hemodynamic alterations verified in the disease,

which is comprehensible since pulmonary arterial remodeling is the most important pathogenic mechanism of MCT-induced PAH. These correlations together with our results make us believe that pulmonary vascular remodeling leads probably to a neurohumoral signaling to the RV inducing survivin overexpression and cardiomyocyte hypertrophy. Some of the molecules that might be responsible for survivin upregulation in the RV are ET-1, angiotensin-II, catecholamines and PDGF<sup>51</sup>. In fact, a positive feedback relationship among PDGF and survivin has been demonstrated to induced SMCs proliferation and apoptosis resistance in arterial injury models<sup>103, 158</sup>. In the future, more studies on the molecular survivin signalling in PAH are needed in order to better understand and comprove this neurohumoral pathway.

The pro-apototic actions of the protein Smac/DIABLO occur from its interaction with IAP proteins preventing their inhibitory effect on caspases<sup>122, 159, 160</sup>. On the other hand, excessive survivin retains Smac/DIABLO in the mitochondria, inhibiting its pro-apoptotic activity<sup>123, 161</sup>. Comparing with RV survivin expression, our molecular and histological results show an inverse pattern of Smac/DIABLO, as it progressively decreases throughout the development of PAH. Thus we suggest that an equilibrium between survivin and Smac/DIABLO could be essential for cardiomyocyte fate in response to apoptotic stimuli. In support of our hypothesis, other groups also demonstrated an antagonism between survivin and Smac/DIABLO in different types of cancers<sup>162-166</sup>.

Although current vasodilation therapies for PAH improve quality of life and survival of patients<sup>167-169</sup>, they don't halt the progression of the disease and therefore there is no cure for PAH available until now<sup>170, 171</sup>. Research is now pursuing strategies that could reverse structural remodelling in the pulmonary arterial bed, thus providing a more significant decrease in pulmonary vascular resistance<sup>151, 152, 172</sup>. The hyperproliferative and apoptosis-resistant phenotype of PASMCs in PAH constitutes a striking therapeutic target. In cancer, several anti-survivin therapies have been tested, being some of them already in clinical trials. For instance, McMurtry<sup>173</sup> demonstrated that delivery gene therapy to inhibit survivin reverted MCT-induced PAH and improved survival. This protein inhibition led to a decrease in proliferation and induced apoptosis of PASMCs without causing systemic alterations<sup>173</sup>. However, pharmacological modulation of survivin in PAH, if similarly effective, would probably be more promptly translated into clinical care than gene therapy. In this context, TMP, an anti-survivin drug, was proven to inhibit proliferation and stimulate apoptosis both *in vitro* and *in vivo* without causing systemic toxicity. Our data demonstrate that modulation of survivin pathway through chronic administration of TMP can be effective on attenuating the pulmonary vascular remodelling with a decrease in the pulmonary artery medial hypertrophy. Interestingly, for the first time, we were able to describe that TMP administration resulted in a fully reversion of RV hypertrophy as well as both systolic and diastolic RV hemodynamic dysfunction. Since no LV alterations were observed, all of these data from the *in vivo* study also support our neurohumoral hypothesis. Finally, in conformity with previous research we also did not registered any systemic alterations when administrating TMP.

Given the lack of therapies aiming remodelling in PAH, our results lead us to believe that TMP would be an interesting pharmacological approach to the treatment of this disease.



## **Part VI – Conclusions**

In the present study it was evaluated the involvement of apoptosis in the pathogenesis of PAH through the expression and modulation of the anti-apoptotic protein survivin. Our data clearly shows survivin overexpression both at cardiac and pulmonary levels of disease animals. Interestingly, the increase in survivin cardiomyocyte expression (and decreasing of the antagonist Smac/DIABLO) was correlated with the beginning of cardiomyocyte hypertrophy. Moreover, both pulmonary and RV survivin overexpression preceded hemodynamic alterations in the RV. This suggests that the deregulation in the balance between apoptosis and survival can be load-independent and due to a compensatory neurohumoral response. Additionally, anti-survivin agent TMP specifically reverted pulmonary and RV remodeling by decreasing both pulmonary medial and cardiomyocyte hypertrophy. The same drug also normalized hemodynamic RV alterations noticed in the disease group. These *in vivo* results demonstrate that TMP may be a potential therapeutic option to PAH.

As future research, we intend to evaluate what type of neurohumoral stimuli is leading to survivin overexpression in PAH. Also relevant would be to understand the specific actions of this protein in PAH by studying its expression in cytoplasmic, nuclear and mitochondrial cellular fractions. Finally, because little is known about the role of survivin in the heart it would be interesting, has future research, to evaluate survivin expression/actions in isolated adult cardiomyocytes of PAH animals.

## Part VII – References



1. Gaine SP, Rubin LJ. Primary pulmonary hypertension. *Lancet*. 1998 Aug 29;352(9129):719-25.
2. Rubin LJ. Pulmonary arterial hypertension. *Proc Am Thorac Soc*. 2006;3(1):111-5.
3. Dresdale DT, Schultz M, Michtom RJ. Primary pulmonary hypertension: I. Clinical and hemodynamic study. *The American Journal of Medicine*. 1951;11(6):686-705.
4. Hatano S, Strasser T. Primary pulmonary hypertension. Report on a WHO meeting, October 15-17, 1973 Geneva: World Health Organization; 1975.
5. McLaughlin VV, Davis M, Cornwell W. Pulmonary arterial hypertension. *Curr Probl Cardiol*. 2011 Dec;36(12):461-517.
6. Simonneau G, Robbins IM, Beghetti M, Channick RN, Delcroix M, Denton CP, et al. Updated clinical classification of pulmonary hypertension. *J Am Coll Cardiol*. 2009 Jun 30;54(1 Suppl):S43-54.
7. Ito T, Ozawa K, Shimada K. Current drug targets and future therapy of pulmonary arterial hypertension. *Curr Med Chem*. 2007;14(6):719-33.
8. Humbert M, Sitbon O, Chaouat A, Bertocchi M, Habib G, Gressin V, et al. Pulmonary arterial hypertension in France: results from a national registry. *Am J Respir Crit Care Med*. 2006 May 1;173(9):1023-30.
9. Peacock AJ, Murphy NF, McMurray JJ, Caballero L, Stewart S. An epidemiological study of pulmonary arterial hypertension. *Eur Respir J*. 2007 Jul;30(1):104-9.
10. Wu SC, Caravita S, Lisi E, Pierini S, Dadone V, Todd SE, et al. Pulmonary arterial hypertension. *Intern Emerg Med*. 2009 Dec;4(6):459-70.
11. Loyd JE, Butler MG, Foroud TM, Conneally PM, Phillips JA, 3rd, Newman JH. Genetic anticipation and abnormal gender ratio at birth in familial primary pulmonary hypertension. *Am J Respir Crit Care Med*. 1995 Jul;152(1):93-7.
12. Fruchter O, Yigla M. Underlying aetiology of pulmonary hypertension in 191 patients: a single centre experience. *Respirology*. 2008 Nov;13(6):825-31.
13. Robbins IM, Newman JH, Johnson RF, Hemnes AR, Fremont RD, Piana RN, et al. Association of the metabolic syndrome with pulmonary venous hypertension. *Chest*. 2009 Jul;136(1):31-6.
14. Butrous G, Ghofrani HA, Grimminger F. Pulmonary vascular disease in the developing world. *Circulation*. 2008 Oct 21;118(17):1758-66.
15. Archer SL, Weir EK, Wilkins MR. Basic science of pulmonary arterial hypertension for clinicians: new concepts and experimental therapies. *Circulation*. 2010 May 11;121(18):2045-66.
16. Pietra GG, Capron F, Stewart S, Leone O, Humbert M, Robbins IM, et al. Pathologic assessment of vasculopathies in pulmonary hypertension. *J Am Coll Cardiol*. 2004 Jun 16;43(12 Suppl S):25S-32S.
17. Tudor RM, Chacon M, Alger L, Wang J, Taraseviciene-Stewart L, Kasahara Y, et al. Expression of angiogenesis-related molecules in plexiform lesions in severe pulmonary hypertension: evidence for a process of disordered angiogenesis. *The Journal of pathology*. 2001 Oct;195(3):367-74.
18. Deng ZM, Morse JH, Slager SL, Cuervo N, Moore KJ, Venetos G, et al. Familial primary pulmonary hypertension (gene PPH1) is caused by mutations in the bone morphogenetic protein receptor-II gene. *American journal of human genetics*. 2000 Sep;67(3):737-44.
19. Lane KB, Machado RD, Pauciulo MW, Thomson JR, Phillips JA, 3rd, Loyd JE, et al. Heterozygous germline mutations in BMPR2, encoding a TGF-beta receptor, cause familial primary pulmonary hypertension. *Nature genetics*. 2000 Sep;26(1):81-4.
20. Austin ED, Loyd JE. Genetics and mediators in pulmonary arterial hypertension. *Clin Chest Med*. 2007 Mar;28(1):43-57, vii-viii.
21. Remillard CV, Tigno DD, Platoshyn O, Burg ED, Brevnova EE, Conger D, et al. Function of Kv1.5 channels and genetic variations of KCNA5 in patients with idiopathic pulmonary arterial hypertension. *Am J Physiol Cell Physiol*. 2007 May;292(5):C1837-53.

22. Yu Y, Keller SH, Remillard CV, Safrina O, Nicholson A, Zhang SL, et al. A functional single-nucleotide polymorphism in the TRPC6 gene promoter associated with idiopathic pulmonary arterial hypertension. *Circulation*. 2009 May 5;119(17):2313-22.
23. Eddahibi S, Chaouat A, Morrell N, Fadel E, Fuhrman C, Bugnet AS, et al. Polymorphism of the serotonin transporter gene and pulmonary hypertension in chronic obstructive pulmonary disease. *Circulation*. 2003 Oct 14;108(15):1839-44.
24. Christman BW, McPherson CD, Newman JH, King GA, Bernard GR, Groves BM, et al. An imbalance between the excretion of thromboxane and prostacyclin metabolites in pulmonary hypertension. *N Engl J Med*. 1992 Jul 9;327(2):70-5.
25. Steudel W, Ichinose F, Huang PL, Hurford WE, Jones RC, Bevan JA, et al. Pulmonary vasoconstriction and hypertension in mice with targeted disruption of the endothelial nitric oxide synthase (NOS 3) gene. *Circ Res*. 1997 Jul;81(1):34-41.
26. Stewart DJ, Levy RD, Cernacek P, Langleben D. Increased plasma endothelin-1 in pulmonary hypertension: marker or mediator of disease? *Ann Intern Med*. 1991 Mar 15;114(6):464-9.
27. White RJ, Meoli DF, Swarthout RF, Kallop DY, Galaria, II, Harvey JL, et al. Plexiform-like lesions and increased tissue factor expression in a rat model of severe pulmonary arterial hypertension. *Am J Physiol Lung Cell Mol Physiol*. 2007 Sep;293(3):L583-90.
28. Sakao S, Tatsumi K, Voelkel NF. Endothelial cells and pulmonary arterial hypertension: apoptosis, proliferation, interaction and transdifferentiation. *Respir Res*. 2009;10:95.
29. Sakao S, Taraseviciene-Stewart L, Lee JD, Wood K, Cool CD, Voelkel NF. Initial apoptosis is followed by increased proliferation of apoptosis-resistant endothelial cells. *FASEB J*. 2005 Jul;19(9):1178-80.
30. Schermuly RT, Dony E, Ghofrani HA, Pullamsetti S, Savai R, Roth M, et al. Reversal of experimental pulmonary hypertension by PDGF inhibition. *J Clin Invest*. 2005 Oct;115(10):2811-21.
31. Eddahibi S, Raffestin B, Hamon M, Adnot S. Is the serotonin transporter involved in the pathogenesis of pulmonary hypertension? *J Lab Clin Med*. 2002 Apr;139(4):194-201.
32. Guignabert C, Izikki M, Tu LI, Li Z, Zadigue P, Barlier-Mur AM, et al. Transgenic mice overexpressing the 5-hydroxytryptamine transporter gene in smooth muscle develop pulmonary hypertension. *Circ Res*. 2006 May 26;98(10):1323-30.
33. Moreno-Vinasco L, Gomberg-Maitland M, Maitland ML, Desai AA, Singleton PA, Sammani S, et al. Genomic assessment of a multikinase inhibitor, sorafenib, in a rodent model of pulmonary hypertension. *Physiol Genomics*. 2008 Apr 22;33(2):278-91.
34. Yuan XJ, Wang J, Juhaszova M, Gaine SP, Rubin LJ. Attenuated K<sup>+</sup> channel gene transcription in primary pulmonary hypertension. *Lancet*. 1998 Mar 7;351(9104):726-7.
35. Cowan KN, Jones PL, Rabinovitch M. Elastase and matrix metalloproteinase inhibitors induce regression, and tenascin-C antisense prevents progression, of vascular disease. *J Clin Invest*. 2000 Jan;105(1):21-34.
36. Welsh DJ, Harnett M, MacLean M, Peacock AJ. Proliferation and signaling in fibroblasts: role of 5-hydroxytryptamine<sub>2A</sub> receptor and transporter. *Am J Respir Crit Care Med*. 2004 Aug 1;170(3):252-9.
37. Bonnet S, Michelakis ED, Porter CJ, Andrade-Navarro MA, Thebaud B, Haromy A, et al. An abnormal mitochondrial-hypoxia inducible factor-1 $\alpha$ -Kv channel pathway disrupts oxygen sensing and triggers pulmonary arterial hypertension in fawn hooded rats: similarities to human pulmonary arterial hypertension. *Circulation*. 2006 Jun 6;113(22):2630-41.
38. Nicolls MR, Taraseviciene-Stewart L, Rai PR, Badesch DB, Voelkel NF. Autoimmunity and pulmonary hypertension: a perspective. *Eur Respir J*. 2005 Dec;26(6):1110-8.



39. Tudor RM, Groves B, Badesch DB, Voelkel NF. Exuberant endothelial cell growth and elements of inflammation are present in plexiform lesions of pulmonary hypertension. *Am J Pathol.* 1994 Feb;144(2):275-85.
40. Isern RA, Yaneva M, Weiner E, Parke A, Rothfield N, Dantzker D, et al. Autoantibodies in patients with primary pulmonary hypertension: association with anti-Ku. *Am J Med.* 1992 Sep;93(3):307-12.
41. Humbert M, Monti G, Brenot F, Sitbon O, Portier A, Grangeot-Keros L, et al. Increased interleukin-1 and interleukin-6 serum concentrations in severe primary pulmonary hypertension. *Am J Respir Crit Care Med.* 1995 May;151(5):1628-31.
42. Cool CD, Rai PR, Yeager ME, Hernandez-Saavedra D, Serls AE, Bull TM, et al. Expression of human herpesvirus 8 in primary pulmonary hypertension. *N Engl J Med.* 2003 Sep 18;349(12):1113-22.
43. Morse JH, Barst RJ, Itescu S, Flaster ER, Sinha G, Zhang Y, et al. Primary pulmonary hypertension in HIV infection: an outcome determined by particular HLA class II alleles. *Am J Respir Crit Care Med.* 1996 Apr;153(4 Pt 1):1299-301.
44. Macian F. NFAT proteins: key regulators of T-cell development and function. *Nat Rev Immunol.* 2005 Jun;5(6):472-84.
45. Rossow CF, Minami E, Chase EG, Murry CE, Santana LF. NFATc3-induced reductions in voltage-gated K<sup>+</sup> currents after myocardial infarction. *Circ Res.* 2004 May 28;94(10):1340-50.
46. Bushdid PB, Osinska H, Waclaw RR, Molkentin JD, Yutzey KE. NFATc3 and NFATc4 are required for cardiac development and mitochondrial function. *Circ Res.* 2003 Jun 27;92(12):1305-13.
47. Bonnet S, Rochefort G, Sutendra G, Archer SL, Haromy A, Webster L, et al. The nuclear factor of activated T cells in pulmonary arterial hypertension can be therapeutically targeted. *Proc Natl Acad Sci U S A.* 2007 Jul 3;104(27):11418-23.
48. Marecki J, Cool C, Voelkel N, Luciw P, Flores S. Evidence for vascular remodeling in the lungs of macaques infected with simian immunodeficiency virus/HIV NEF recombinant virus. *Chest.* 2005 Dec;128(6 Suppl):621S-2S.
49. Marecki JC, Cool CD, Parr JE, Beckey VE, Luciw PA, Tarantal AF, et al. HIV-1 Nef is associated with complex pulmonary vascular lesions in SHIV-nef-infected macaques. *Am J Respir Crit Care Med.* 2006 Aug 15;174(4):437-45.
50. Crosby A, Jones FM, Southwood M, Stewart S, Schermuly R, Butrous G, et al. Pulmonary vascular remodeling correlates with lung eggs and cytokines in murine schistosomiasis. *Am J Respir Crit Care Med.* 2010 Feb 1;181(3):279-88.
51. Bogaard HJ, Abe K, Vonk Noordegraaf A, Voelkel NF. The right ventricle under pressure: cellular and molecular mechanisms of right-heart failure in pulmonary hypertension. *Chest.* 2009 Mar;135(3):794-804.
52. Haworth SG. The cell and molecular biology of right ventricular dysfunction in pulmonary hypertension. *European Heart Journal Supplements.* 2007 December 2007;9(suppl H):H10-H6.
53. Nagendran J, Archer SL, Soliman D, Gurtu V, Moudgil R, Haromy A, et al. Phosphodiesterase type 5 is highly expressed in the hypertrophied human right ventricle, and acute inhibition of phosphodiesterase type 5 improves contractility. *Circulation.* 2007 Jul 17;116(3):238-48.
54. Piao L, Fang YH, Cadete VJ, Wietholt C, Urboniene D, Toth PT, et al. The inhibition of pyruvate dehydrogenase kinase improves impaired cardiac function and electrical remodeling in two models of right ventricular hypertrophy: resuscitating the hibernating right ventricle. *J Mol Med (Berl).* 2010 Jan;88(1):47-60.
55. Broderick TL, King TM. Upregulation of GLUT-4 in right ventricle of rats with monocrotaline-induced pulmonary hypertension. *Med Sci Monit.* 2008 Dec;14(12):BR261-4.

56. Campian ME, Hardziyenka M, Michel MC, Tan HL. How valid are animal models to evaluate treatments for pulmonary hypertension? *Naunyn Schmiedebergs Arch Pharmacol*. 2006 Sep;373(6):391-400.
57. Robbins IM. Advancing therapy for pulmonary arterial hypertension: can animal models help? *Am J Respir Crit Care Med*. 2004 Jan 1;169(1):5-6.
58. Lalic JJ, Merkow L. Pulmonary arteritis produced in rat by feeding *Crotalaria spectabilis*. *Lab Invest*. 1961 Jul-Aug;10:744-50.
59. Mattocks AR. Toxicity of pyrrolizidine alkaloids. *Nature*. 1968 Feb 24;217(5130):723-8.
60. Urboniene D, Haber I, Fang YH, Thenappan T, Archer SL. Validation of high-resolution echocardiography and magnetic resonance imaging vs. high-fidelity catheterization in experimental pulmonary hypertension. *Am J Physiol Lung Cell Mol Physiol*. 2010 Sep;299(3):L401-12.
61. Kay JM, Smith P, Heath D. Electron microscopy of *Crotalaria* pulmonary hypertension. *Thorax*. 1969 Sep;24(5):511-26.
62. Schoental R, Head MA. Pathological changes in rats as a result of treatment with monocrotaline. *Br J Cancer*. 1955 Mar;9(1):229-37.
63. Hardziyenka M, Campian ME, de Bruin-Bon HA, Michel MC, Tan HL. Sequence of echocardiographic changes during development of right ventricular failure in rat. *J Am Soc Echocardiogr*. 2006 Oct;19(10):1272-9.
64. Plestina R, Stoner HB. Pulmonary oedema in rats given monocrotaline pyrrole. *J Pathol*. 1972 Apr;106(4):235-49.
65. Lalic JL, Johnson WD, Racznik TJ, Shumaker RC. Fibrin thrombosis in monocrotaline pyrrole-induced cor pulmonale in rats. *Arch Pathol Lab Med*. 1977 Feb;101(2):69-73.
66. Rosenberg HC, Rabinovitch M. Endothelial injury and vascular reactivity in monocrotaline pulmonary hypertension. *Am J Physiol*. 1988 Dec;255(6 Pt 2):H1484-91.
67. Ryan J, Bloch K, Archer SL. Rodent models of pulmonary hypertension: harmonisation with the world health organisation's categorisation of human PH. *Int J Clin Pract Suppl*. 2011 Aug(172):15-34.
68. Meyrick B, Gamble W, Reid L. Development of *Crotalaria* pulmonary hypertension: hemodynamic and structural study. *Am J Physiol*. 1980 Nov;239(5):H692-702.
69. Brown L, Miller J, Dagger A, Sernia C. Cardiac and vascular responses after monocrotaline-induced hypertrophy in rats. *J Cardiovasc Pharmacol*. 1998 Jan;31(1):108-15.
70. Hessel MH, Steendijk P, den Adel B, Schutte CI, van der Laarse A. Characterization of right ventricular function after monocrotaline-induced pulmonary hypertension in the intact rat. *Am J Physiol Heart Circ Physiol*. 2006 Nov;291(5):H2424-30.
71. Werchan PM, Summer WR, Gerdes AM, McDonough KH. Right ventricular performance after monocrotaline-induced pulmonary hypertension. *Am J Physiol*. 1989 May;256(5 Pt 2):H1328-36.
72. Intengan HD, Schiffrin EL. Vascular remodeling in hypertension: roles of apoptosis, inflammation, and fibrosis. *Hypertension*. 2001 Sep;38(3 Pt 2):581-7.
73. Hengartner MO. The biochemistry of apoptosis. *Nature*. 2000 Oct 12;407(6805):770-6.
74. Okada Y, Maeno E, Shimizu T, Dezaki K, Wang J, Morishima S. Receptor-mediated control of regulatory volume decrease (RVD) and apoptotic volume decrease (AVD). *J Physiol*. 2001 Apr 1;532(Pt 1):3-16.
75. Zimmermann KC, Bonzon C, Green DR. The machinery of programmed cell death. *Pharmacol Ther*. 2001 Oct;92(1):57-70.
76. Slee EA, Adrain C, Martin SJ. Executioner caspase-3, -6, and -7 perform distinct, non-redundant roles during the demolition phase of apoptosis. *J Biol Chem*. 2001 Mar 9;276(10):7320-6.
77. Locksley RM, Killeen N, Lenardo MJ. The TNF and TNF receptor superfamilies: integrating mammalian biology. *Cell*. 2001 Feb 23;104(4):487-501.

78. Ashkenazi A, Dixit VM. Death receptors: signaling and modulation. *Science*. 1998 Aug 28;281(5381):1305-8.
79. Chicheportiche Y, Bourdon PR, Xu H, Hsu YM, Scott H, Hession C, et al. TWEAK, a new secreted ligand in the tumor necrosis factor family that weakly induces apoptosis. *J Biol Chem*. 1997 Dec 19;272(51):32401-10.
80. Peter ME, Krammer PH. Mechanisms of CD95 (APO-1/Fas)-mediated apoptosis. *Curr Opin Immunol*. 1998 Oct;10(5):545-51.
81. Rubio-Moscardo F, Blesa D, Mestre C, Siebert R, Balasas T, Benito A, et al. Characterization of 8p21.3 chromosomal deletions in B-cell lymphoma: TRAIL-R1 and TRAIL-R2 as candidate dosage-dependent tumor suppressor genes. *Blood*. 2005 Nov 1;106(9):3214-22.
82. Suliman A, Lam A, Datta R, Srivastava RK. Intracellular mechanisms of TRAIL: apoptosis through mitochondrial-dependent and -independent pathways. *Oncogene*. 2001 Apr 19;20(17):2122-33.
83. Kischkel FC, Hellbardt S, Behrmann I, Germer M, Pawlita M, Krammer PH, et al. Cytotoxicity-dependent APO-1 (Fas/CD95)-associated proteins form a death-inducing signaling complex (DISC) with the receptor. *EMBO J*. 1995 Nov 15;14(22):5579-88.
84. Saelens X, Festjens N, Vande Walle L, van Gurp M, van Loo G, Vandenabeele P. Toxic proteins released from mitochondria in cell death. *Oncogene*. 2004 Apr 12;23(16):2861-74.
85. Chinnaiyan AM. The apoptosome: heart and soul of the cell death machine. *Neoplasia*. 1999 Apr;1(1):5-15.
86. Hill MM, Adrain C, Duriez PJ, Creagh EM, Martin SJ. Analysis of the composition, assembly kinetics and activity of native Apaf-1 apoptosomes. *EMBO J*. 2004 May 19;23(10):2134-45.
87. Cory S, Adams JM. The Bcl2 family: regulators of the cellular life-or-death switch. *Nat Rev Cancer*. 2002 Sep;2(9):647-56.
88. Gulbins E, Jekle A, Ferlinz K, Grassme H, Lang F. Physiology of apoptosis. *Am J Physiol Renal Physiol*. 2000 Oct;279(4):F605-15.
89. Shimizu S, Tsujimoto Y. Proapoptotic BH3-only Bcl-2 family members induce cytochrome c release, but not mitochondrial membrane potential loss, and do not directly modulate voltage-dependent anion channel activity. *Proc Natl Acad Sci U S A*. 2000 Jan 18;97(2):577-82.
90. Remillard CV, Yuan JX. Activation of K<sup>+</sup> channels: an essential pathway in programmed cell death. *Am J Physiol Lung Cell Mol Physiol*. 2004 Jan;286(1):L49-67.
91. Bortner CD, Hughes FM, Jr., Cidlowski JA. A primary role for K<sup>+</sup> and Na<sup>+</sup> efflux in the activation of apoptosis. *J Biol Chem*. 1997 Dec 19;272(51):32436-42.
92. Fadok VA, Chimini G. The phagocytosis of apoptotic cells. *Semin Immunol*. 2001 Dec;13(6):365-72.
93. Rabinovitch M. Elastase and the pathobiology of unexplained pulmonary hypertension. *Chest*. 1998 Sep;114(3 Suppl):213S-24S.
94. Irani K. Oxidant signaling in vascular cell growth, death, and survival : a review of the roles of reactive oxygen species in smooth muscle and endothelial cell mitogenic and apoptotic signaling. *Circ Res*. 2000 Aug 4;87(3):179-83.
95. Pollman MJ, Yamada T, Horiuchi M, Gibbons GH. Vasoactive substances regulate vascular smooth muscle cell apoptosis. Countervailing influences of nitric oxide and angiotensin II. *Circ Res*. 1996 Oct;79(4):748-56.
96. Yamada T, Horiuchi M, Dzau VJ. Angiotensin II type 2 receptor mediates programmed cell death. *Proc Natl Acad Sci U S A*. 1996 Jan 9;93(1):156-60.
97. Cattaruzza M, Dimigen C, Ehrenreich H, Hecker M. Stretch-induced endothelin B receptor-mediated apoptosis in vascular smooth muscle cells. *FASEB J*. 2000 May;14(7):991-8.

98. Li PF, Maasch C, Haller H, Dietz R, von Harsdorf R. Requirement for protein kinase C in reactive oxygen species-induced apoptosis of vascular smooth muscle cells. *Circulation*. 1999 Aug 31;100(9):967-73.
99. Cowan KN, Heilbut A, Humpl T, Lam C, Ito S, Rabinovitch M. Complete reversal of fatal pulmonary hypertension in rats by a serine elastase inhibitor. *Nat Med*. 2000 Jun;6(6):698-702.
100. Cowan KN, Jones PL, Rabinovitch M. Regression of hypertrophied rat pulmonary arteries in organ culture is associated with suppression of proteolytic activity, inhibition of tenascin-C, and smooth muscle cell apoptosis. *Circ Res*. 1999 May 28;84(10):1223-33.
101. Weir EK, Archer SL. The mechanism of acute hypoxic pulmonary vasoconstriction: the tale of two channels. *FASEB J*. 1995 Feb;9(2):183-9.
102. Durmowicz AG, Stenmark KR. Mechanisms of structural remodeling in chronic pulmonary hypertension. *Pediatr Rev*. 1999 Nov;20(11):e91-e102.
103. Blanc-Brude OP, Yu J, Simosa H, Conte MS, Sessa WC, Altieri DC. Inhibitor of apoptosis protein survivin regulates vascular injury. *Nat Med*. 2002 Sep;8(9):987-94.
104. Bjorkerud S, Bjorkerud B, Joelsson M. Structural organization of reconstituted human arterial smooth muscle tissue. *Arterioscler Thromb*. 1994 Apr;14(4):644-51.
105. Seidl R, Bajo M, Bohm K, LaCasse EC, MacKenzie AE, Cairns N, et al. Neuronal apoptosis inhibitory protein (NAIP)-like immunoreactivity in brains of adult patients with Down syndrome. *J Neural Transm Suppl*. 1999;57:283-91.
106. Wagenknecht B, Glaser T, Naumann U, Kugler S, Isenmann S, Bahr M, et al. Expression and biological activity of X-linked inhibitor of apoptosis (XIAP) in human malignant glioma. *Cell Death Differ*. 1999 Apr;6(4):370-6.
107. Vucic D, Stennicke HR, Pisabarro MT, Salvesen GS, Dixit VM. ML-IAP, a novel inhibitor of apoptosis that is preferentially expressed in human melanomas. *Curr Biol*. 2000 Nov 2;10(21):1359-66.
108. Kasof GM, Gomes BC. Livin, a novel inhibitor of apoptosis protein family member. *J Biol Chem*. 2001 Feb 2;276(5):3238-46.
109. Ashhab Y, Alian A, Polliack A, Panet A, Ben Yehuda D. Two splicing variants of a new inhibitor of apoptosis gene with different biological properties and tissue distribution pattern. *FEBS Lett*. 2001 Apr 20;495(1-2):56-60.
110. Altieri DC, Marchisio PC. Survivin apoptosis: an interloper between cell death and cell proliferation in cancer. *Lab Invest*. 1999 Nov;79(11):1327-33.
111. Ambrosini G, Adida C, Altieri DC. A novel anti-apoptosis gene, survivin, expressed in cancer and lymphoma. *Nat Med*. 1997 Aug;3(8):917-21.
112. Guo M, Hay BA. Cell proliferation and apoptosis. *Curr Opin Cell Biol*. 1999 Dec;11(6):745-52.
113. Buolamwini JK. Novel anticancer drug discovery. *Curr Opin Chem Biol*. 1999 Aug;3(4):500-9.
114. Altieri DC. The molecular basis and potential role of survivin in cancer diagnosis and therapy. *Trends Mol Med*. 2001 Dec;7(12):542-7.
115. Adida C, Crotty PL, McGrath J, Berrebi D, Diebold J, Altieri DC. Developmentally regulated expression of the novel cancer anti-apoptosis gene survivin in human and mouse differentiation. *Am J Pathol*. 1998 Jan;152(1):43-9.
116. Velculescu VE, Madden SL, Zhang L, Lash AE, Yu J, Rago C, et al. Analysis of human transcriptomes. *Nat Genet*. 1999 Dec;23(4):387-8.
117. Deveraux QL, Reed JC. IAP family proteins--suppressors of apoptosis. *Genes Dev*. 1999 Feb 1;13(3):239-52.
118. Dohi T, Okada K, Xia F, Wilford CE, Samuel T, Welsh K, et al. An IAP-IAP complex inhibits apoptosis. *J Biol Chem*. 2004 Aug 13;279(33):34087-90.

119. O'Connor DS, Grossman D, Plescia J, Li F, Zhang H, Villa A, et al. Regulation of apoptosis at cell division by p34cdc2 phosphorylation of survivin. *Proc Natl Acad Sci U S A*. 2000 Nov 21;97(24):13103-7.
120. Mesri M, Wall NR, Li J, Kim RW, Altieri DC. Cancer gene therapy using a survivin mutant adenovirus. *J Clin Invest*. 2001 Oct;108(7):981-90.
121. Guo F, Nimmanapalli R, Paranawithana S, Wittman S, Griffin D, Bali P, et al. Ectopic overexpression of second mitochondria-derived activator of caspases (Smac/DIABLO) or cotreatment with N-terminus of Smac/DIABLO peptide potentiates epothilone B derivative-(BMS 247550) and Apo-2L/TRAIL-induced apoptosis. *Blood*. 2002 May 1;99(9):3419-26.
122. Du C, Fang M, Li Y, Li L, Wang X. Smac, a mitochondrial protein that promotes cytochrome c-dependent caspase activation by eliminating IAP inhibition. *Cell*. 2000 Jul 7;102(1):33-42.
123. Ceballos-Cancino G, Espinosa M, Maldonado V, Melendez-Zajgla J. Regulation of mitochondrial Smac/DIABLO-selective release by survivin. *Oncogene*. 2007 Nov 29;26(54):7569-75.
124. Mahotka C, Wenzel M, Springer E, Gabbert HE, Gerharz CD. Survivin-deltaEx3 and survivin-2B: two novel splice variants of the apoptosis inhibitor survivin with different antiapoptotic properties. *Cancer Res*. 1999 Dec 15;59(24):6097-102.
125. Caldas H, Jiang Y, Holloway MP, Fangusaro J, Mahotka C, Conway EM, et al. Survivin splice variants regulate the balance between proliferation and cell death. *Oncogene*. 2005 Mar 17;24(12):1994-2007.
126. Badran A, Yoshida A, Ishikawa K, Goi T, Yamaguchi A, Ueda T, et al. Identification of a novel splice variant of the human anti-apoptosis gene survivin. *Biochem Biophys Res Commun*. 2004 Feb 13;314(3):902-7.
127. Srinivasula SM, Ashwell JD. IAPs: what's in a name? *Mol Cell*. 2008 Apr 25;30(2):123-35.
128. Uren AG, Wong L, Pakusch M, Fowler KJ, Burrows FJ, Vaux DL, et al. Survivin and the inner centromere protein INCENP show similar cell-cycle localization and gene knockout phenotype. *Curr Biol*. 2000 Nov 2;10(21):1319-28.
129. Li F, Ambrosini G, Chu EY, Plescia J, Tognin S, Marchisio PC, et al. Control of apoptosis and mitotic spindle checkpoint by survivin. *Nature*. 1998 Dec 10;396(6711):580-4.
130. Kelly AE, Ghenoiu C, Xue JZ, Zierhut C, Kimura H, Funabiki H. Survivin reads phosphorylated histone H3 threonine 3 to activate the mitotic kinase Aurora B. *Science*. 2010 Oct 8;330(6001):235-9.
131. Fortugno P, Wall NR, Giodini A, O'Connor DS, Plescia J, Padgett KM, et al. Survivin exists in immunochemically distinct subcellular pools and is involved in spindle microtubule function. *J Cell Sci*. 2002 Feb 1;115(Pt 3):575-85.
132. Dohi T, Beltrami E, Wall NR, Plescia J, Altieri DC. Mitochondrial survivin inhibits apoptosis and promotes tumorigenesis. *J Clin Invest*. 2004 Oct;114(8):1117-27.
133. Temme A, Rodriguez JA, Hendruschik S, Gunes S, Weigle B, Schakel K, et al. Nuclear localization of Survivin renders HeLa tumor cells more sensitive to apoptosis by induction of p53 and Bax. *Cancer Lett*. 2007 Jun 8;250(2):177-93.
134. Connell CM, Wheatley SP, McNeish IA. Nuclear survivin abrogates multiple cell cycle checkpoints and enhances viral oncolysis. *Cancer Res*. 2008 Oct 1;68(19):7923-31.
135. Connell CM, Colnaghi R, Wheatley SP. Nuclear survivin has reduced stability and is not cytoprotective. *J Biol Chem*. 2008 Feb 8;283(6):3289-96.
136. Dohi T, Altieri DC. Mitochondrial dynamics of survivin and "four dimensional" control of tumor cell apoptosis. *Cell Cycle*. 2005 Jan;4(1):21-3.
137. Mera S, Magnusson M, Tarkowski A, Bokarewa M. Extracellular survivin up-regulates adhesion molecules on the surface of leukocytes changing their reactivity pattern. *J Leukoc Biol*. 2008 Jan;83(1):149-55.

138. Khan S, Aspe JR, Asumen MG, Almaguel F, Odumosu O, Acevedo-Martinez S, et al. Extracellular, cell-permeable survivin inhibits apoptosis while promoting proliferative and metastatic potential. *Br J Cancer*. 2009 Apr 7;100(7):1073-86.
139. Bokarewa M, Lindblad S, Bokarew D, Tarkowski A. Balance between survivin, a key member of the apoptosis inhibitor family, and its specific antibodies determines erosivity in rheumatoid arthritis. *Arthritis Res Ther*. 2005;7(2):R349-58.
140. Chen Q. Nordihydroguaiaretic acid analogues: their chemical synthesis and biological activities. *Curr Top Med Chem*. 2009;9(17):1636-59.
141. Hwu JR, Tseng WN, Gnabre J, Giza P, Huang RC. Antiviral activities of methylated nordihydroguaiaretic acids. 1. Synthesis, structure identification, and inhibition of tat-regulated HIV transactivation. *J Med Chem*. 1998 Jul 30;41(16):2994-3000.
142. Chang CC, Heller JD, Kuo J, Huang RC. Tetra-O-methyl nordihydroguaiaretic acid induces growth arrest and cellular apoptosis by inhibiting Cdc2 and survivin expression. *Proc Natl Acad Sci U S A*. 2004 Sep 7;101(36):13239-44.
143. Park R, Chang CC, Liang YC, Chung Y, Henry RA, Lin E, et al. Systemic treatment with tetra-O-methyl nordihydroguaiaretic acid suppresses the growth of human xenograft tumors. *Clin Cancer Res*. 2005 Jun 15;11(12):4601-9.
144. Fulciniti M, Amin S, Nanjappa P, Rodig S, Prabhala R, Li C, et al. Significant biological role of sp1 transactivation in multiple myeloma. *Clin Cancer Res*. 2011 Oct 15;17(20):6500-9.
145. Heller JD, Kuo J, Wu TC, Kast WM, Huang RC. Tetra-O-methyl nordihydroguaiaretic acid induces G2 arrest in mammalian cells and exhibits tumoricidal activity in vivo. *Cancer Res*. 2001 Jul 15;61(14):5499-504.
146. Lambert JD, Meyers RO, Timmermann BN, Dorr RT. tetra-O-methylnordihydroguaiaretic acid inhibits melanoma in vivo. *Cancer Lett*. 2001 Sep 28;171(1):47-56.
147. Lopez RA, Goodman AB, Rhodes M, Blomberg JA, Heller J. The anticancer activity of the transcription inhibitor terameprocol (meso-tetra-O-methyl nordihydroguaiaretic acid) formulated for systemic administration. *Anticancer Drugs*. 2007 Sep;18(8):933-9.
148. Ng SB, Selvarajan V, Huang G, Zhou J, Feldman AL, Law M, et al. Activated oncogenic pathways and therapeutic targets in extranodal nasal-type NK/T cell lymphoma revealed by gene expression profiling. *J Pathol*. 2011 Mar;223(4):496-510.
149. Pacher P, Mabley JG, Liaudet L, Evgenov OV, Marton A, Hasko G, et al. Left ventricular pressure-volume relationship in a rat model of advanced aging-associated heart failure. *Am J Physiol Heart Circ Physiol*. 2004 Nov;287(5):H2132-7.
150. Laemmli UK. Cleavage of structural proteins during the assembly of the head of bacteriophage T4. *Nature*. 1970 Aug 15;227(5259):680-5.
151. Huang JB, Liu YL, Sun PW, Lv XD, Bo K, Fan XM. Novel strategy for treatment of pulmonary arterial hypertension: enhancement of apoptosis. *Lung*. 2010 Jun;188(3):179-89.
152. Rubin LJ. Therapy of pulmonary hypertension: the evolution from vasodilators to antiproliferative agents. *Am J Respir Crit Care Med*. 2002 Nov 15;166(10):1308-9.
153. Altieri DC. Survivin, versatile modulation of cell division and apoptosis in cancer. *Oncogene*. 2003 Nov 24;22(53):8581-9.
154. Santini D, Abbate A, Scarpa S, Vasaturo F, Biondi-Zoccai GG, Bussani R, et al. Surviving acute myocardial infarction: survivin expression in viable cardiomyocytes after infarction. *J Clin Pathol*. 2004 Dec;57(12):1321-4.
155. Fukuda S, Kaga S, Sasaki H, Zhan L, Zhu L, Otani H, et al. Angiogenic signal triggered by ischemic stress induces myocardial repair in rat during chronic infarction. *J Mol Cell Cardiol*. 2004 Apr;36(4):547-59.

156. Abbate A, Scarpa S, Santini D, Palleiro J, Vasaturo F, Miller J, et al. Myocardial expression of survivin, an apoptosis inhibitor, in aging and heart failure. An experimental study in the spontaneously hypertensive rat. *Int J Cardiol.* 2006 Aug 28;111(3):371-6.
157. Levkau B, Schafer M, Wohlschlaeger J, von Wnuck Lipinski K, Keul P, Hermann S, et al. Survivin determines cardiac function by controlling total cardiomyocyte number. *Circulation.* 2008 Mar 25;117(12):1583-93.
158. Wang GJ, Sui XX, Simosa HF, Jain MK, Altieri DC, Conte MS. Regulation of vein graft hyperplasia by survivin, an inhibitor of apoptosis protein. *Arterioscler Thromb Vasc Biol.* 2005 Oct;25(10):2081-7.
159. Verhagen AM, Ekert PG, Pakusch M, Silke J, Connolly LM, Reid GE, et al. Identification of DIABLO, a mammalian protein that promotes apoptosis by binding to and antagonizing IAP proteins. *Cell.* 2000 Jul 7;102(1):43-53.
160. Sun C, Nettesheim D, Liu Z, Olejniczak ET. Solution structure of human survivin and its binding interface with Smac/Diablo. *Biochemistry.* 2005 Jan 11;44(1):11-7.
161. Song Z, Yao X, Wu M. Direct interaction between survivin and Smac/DIABLO is essential for the anti-apoptotic activity of survivin during taxol-induced apoptosis. *J Biol Chem.* 2003 Jun 20;278(25):23130-40.
162. Gao Y, Zhang H, Zhang M, Yu X, Kong W, Zha X, et al. N-terminal deletion effects of human survivin on dimerization and binding to Smac/DIABLO in vitro. *J Phys Chem B.* 2010 Dec 2;114(47):15656-62.
163. Mansour A, Nabil M, Ali-Labib R, Said H, Annos F. Reciprocal expression of survivin and SMAC/DIABLO in primary breast cancer. *Med Oncol.* 2012 Dec;29(4):2535-42.
164. McNeish IA, Lopes R, Bell SJ, McKay TR, Fernandez M, Lockley M, et al. Survivin interacts with Smac/DIABLO in ovarian carcinoma cells but is redundant in Smac-mediated apoptosis. *Exp Cell Res.* 2005 Jan 1;302(1):69-82.
165. Ogura A, Watanabe Y, Iizuka D, Yasui H, Amitani M, Kobayashi S, et al. Radiation-induced apoptosis of tumor cells is facilitated by inhibition of the interaction between Survivin and Smac/DIABLO. *Cancer Lett.* 2008 Jan 18;259(1):71-81.
166. Oikawa T, Unno Y, Matsuno K, Sawada J, Ogo N, Tanaka K, et al. Identification of a small-molecule inhibitor of the interaction between Survivin and Smac/DIABLO. *Biochem Biophys Res Commun.* 2010;393(2):253-8.
167. Galie N, Humbert M, Vachieri JL, Vizza CD, Kneussl M, Manes A, et al. Effects of beraprost sodium, an oral prostacyclin analogue, in patients with pulmonary arterial hypertension: a randomized, double-blind, placebo-controlled trial. *J Am Coll Cardiol.* 2002 May 1;39(9):1496-502.
168. Rubin LJ, Badesch DB, Barst RJ, Galie N, Black CM, Keogh A, et al. Bosentan therapy for pulmonary arterial hypertension. *N Engl J Med.* 2002 Mar 21;346(12):896-903.
169. Schermuly RT, Kreisselmeier KP, Ghofrani HA, Yilmaz H, Butrous G, Ermert L, et al. Chronic sildenafil treatment inhibits monocrotaline-induced pulmonary hypertension in rats. *Am J Respir Crit Care Med.* 2004 Jan 1;169(1):39-45.
170. Farber HWaJL. Pulmonary arterial hypertension. *N Engl J Med.* 2004;351(16):1655-65.
171. Humbert M, Sitbon O, Simonneau G. Treatment of pulmonary arterial hypertension. *N Engl J Med.* 2004 Sep 30;351(14):1425-36.
172. Jurasz P, Courtman D, Babaie S, Stewart DJ. Role of apoptosis in pulmonary hypertension: from experimental models to clinical trials. *Pharmacol Ther.* 2010 Apr;126(1):1-8.
173. McMurtry MS, Archer SL, Altieri DC, Bonnet S, Haromy A, Harry G, et al. Gene therapy targeting survivin selectively induces pulmonary vascular apoptosis and reverses pulmonary arterial hypertension. *J Clin Invest.* 2005 Jun;115(6):1479-91.